A multi-component, multi-species model of vegetation–atmosphere CO_2 and energy exchange for mountain grasslands

G. Wohlfahrt [a,b,*], M. Bahn [a], U. Tappeiner [a,c], A. Cernusca [a]

[a] *Institut für Botanik, Universität Innsbruck, Sternwartestr. 15, 6020 Innsbruck, Austria*
[b] *Centro di Ecologia Alpina, Viote del Monte Bondone, 38040 Trento, Italy*
[c] *Europäische Akademie Bozen, Domplatz 3, 39100 Bolzano, Italy*

Abstract

A model is presented which allows simulation of vegetation–atmosphere CO_2 and energy exchange of multi-component, multi-species canopies, explicitly taking into account the structural and functional properties of the various components and species. The model is parameterised for a meadow and an abandoned area at the ECOMONT study area Monte Bondone (1500 m a.s.l., Trento/Italy). A series of sensitivity tests showed the model to be sensitive to vegetation optical and physiological properties, but not to soil optical properties, dwarf shrub bole respiration parameters and phytoelement inclination and width. Validation of canopy CO_2 and energy exchange rates against the respective fluxes measured by the means of the Bowen-ratio-energy-balance method yields broadly satisfactory results. Though it proves difficult to validate canopy latent and sensible heat flux, due to the fact that the vegetation–atmosphere-transfer model does not include contributions by the soil, whereas measured fluxes do, indicating both the need for further model development as well as experimental studies. Finally, the model is used to test for the effects of simplifications in input data likely to occur when being applied at larger spatial and/or temporal scales. © 2001 Elsevier Science B.V. All rights reserved.

1. Introduction

The rates at which CO_2 and energy are exchanged between the biosphere and atmosphere continues to be a subject of active research, motivated by fundamental environmental changes occurring on our planet (e.g. Steffen et al., 1998; Lloyd, 1999; Running et al., 1999). In order to arrive at an understanding of the processes controlling biosphere–atmosphere exchange, modelling studies play an important role, since model simulations allow to test future scenarios, to separate various component processes, and to study their interaction (Ehleringer and Field, 1993; Van Gardingen et al., 1997; Cernusca et al., 1998).

Two major approaches of representing the vegetation component of the land surface may be distinguished (Raupach and Finnigan, 1988): one line of models treats the vegetation as if it was a single "big leaf", possibly distinguishing between a sunlit and a shaded fraction (De Pury and Farquhar, 1997; Wang and Leuning, 1998; Kellomäki and Wang, 1999;

* Corresponding author. Present address: Institut für Botanik, Universität Innsbruck, Sternwartestr. 15, 6020 Innsbruck, Austria. Tel.: +43-512-507-5917; fax: +43-512-507-2975.
E-mail address: georg.wohlfahrt@uibk.ac.at (G. Wohlfahrt).

Nomenclature

A	net photosynthesis (μmol m^{-2} s^{-1})
A_C	canopy net photosynthesis (μmol m^{-2} s^{-1})
B_l	normalised view factor (–)
B_u	zonal distribution of scattered and emitted radiation (–)
BREB	Bowen-ratio-energy-balance method
c_p	specific heat of dry air (1010 J kg^{-1} K^{-1})
C_a	CO_2 concentration of ambient air (μmol mol^{-1})
C_i	CO_2 concentration in the intercellular space (μmol mol^{-1})
C_s	CO_2 concentration at the leaf surface (μmol mol^{-1})
CRY	cryptogams
DgS, DngS	green and non-green stems of dwarf shrubs
DL	dwarf shrub leaves
e_a	air water vapour pressure (hPa)
$e_s(T)$	saturated leaf water vapour pressure (hPa)
f_{sl}	fraction of sunlit phytoelements (–)
F	phytoelement inclination distribution (–)
F_C	CO_2 flux above the canopy (μmol m^{-2} s^{-1})
FL, FS	forb leaves and stems, respectively
FRU	fruits
g_{bv}	all-sided boundary layer conductance to water vapour (mmol m^{-2} s^{-1})
g_{min}	minimum stomatal conductance to water vapour (mmol m^{-2} s^{-1})
g_{sv}	stomatal conductance to water vapour (mmol m^{-2} s^{-1})
g_{tv}	total conductance to water vapour (mmol m^{-2} s^{-1})
GAI	green area index (m^2 m^{-2})
$G(\beta, \lambda)$	projection of leaves with inclination λ into inclination β (–)
G_{fac}	stomatal sensitivity coefficient (–)
GCM	global circulation model
GL, GS	graminoid leaves and stems, respectively
h_s	leaf surface relative humidity (–)
H	sensible heat loss (W m^{-2})
ΔH_a	energy of activation (J mol^{-1})
ΔH_d	energy of deactivation (J mol^{-1})
I_{fac}	coefficient representing the extent to which R_{dark} is inhibited in the light (–)
INF	inflorescences
IR	long-wave radiation (W m^{-2})
j	subscript indicating canopy layer
L	long-wave radiation incident on phytoelements (W m^{-2})
ΔL	PAI in canopy layer (m^2 m^{-2})
L_d	downward flux of long-wave radiation (W m^{-2})
L_e	emitted long-wave radiation (W m^{-2})
L_u	upward flux of long-wave radiation (W m^{-2})
LAI	leaf area index (m^2 m^{-2})
LE	latent heat loss (W m^{-2})
n	number of canopy layers

np	number of species
NEC	attached dead plant material
NIR	near infrared radiation ($W\,m^{-2}$)
O_i	O_2 concentration in the intercellular space ($mmol\,mol^{-1}$)
p	subscript indicating species
P_i	probability of interception (–)
P_{ml}	potential rate of RuBP regeneration ($\mu mol\,m^{-2}\,s^{-1}$)
PAI	plant area index ($m^2\,m^{-2}$)
PPFD	photosynthetic photon flux density ($\mu mol\,m^{-2}\,s^{-1}$)
Q_d	downward flux of diffuse short-wave radiation ($W\,m^{-2}$)
Q_{dir}	downward flux of beam radiation ($W\,m^{-2}$)
Q_{shade}	short-wave radiation incident on shaded phytoelements ($W\,m^{-2}$)
Q_{solar}	incident short-wave radiation ($W\,m^{-2}$)
Q_{sun}	short-wave radiation incident on sunlit phytoelements ($W\,m^{-2}$)
Q_u	upward flux of diffuse short-wave radiation ($W\,m^{-2}$)
R	universal gas constant ($8.314\,m^3\,Pa\,mol^{-1}\,K^{-1}$)
R_{abs}	bi-directional absorbed short-wave and long-wave radiation ($W\,m^{-2}$)
R_{bole}	bole respiration ($\mu mol\,m^{-2}\,s^{-1}$)
R_{dark}	dark respiration rate ($\mu mol\,m^{-2}\,s^{-1}$)
R_{day}	respiration rate during day light ($\mu mol\,m^{-2}\,s^{-1}$)
R_N	net radiation (soil + vegetation) ($W\,m^{-2}$)
R_{Nveg}	vegetation net radiation ($R_N - $ soil net radiation) ($W\,m^{-2}$)
R_{soil}	soil respiration ($\mu mol\,m^{-2}\,s^{-1}$)
RUBISCO	ribulose-1,5-bisphosphate carboxylase/oxygenase
RuBP	ribulose-1,5-bisphosphate
S	soil heat flux ($W\,m^{-2}$)
ΔS	entropy term ($J\,K^{-1}\,mol^{-1}$)
T_a	air temperature ($^\circ C$)
T_p	phytoelement temperature ($^\circ C$)
T_{pK}	phytoelement temperature (K)
T_{pKsh}	phytoelement temperature of shaded leaves (K)
T_{pKsl}	phytoelement temperature of sunlit leaves (K)
T_{ref}	reference temperature (273.16 K)
T_s	soil surface temperature ($^\circ C$)
T_{sK}	soil surface temperature (K)
V_{Cmax}	maximum rate of carboxylation ($\mu mol\,m^{-2}\,s^{-1}$)
VAT	vegetation–atmosphere-transfer
W_C	RuBP-saturated rate of carboxylation ($\mu mol\,m^{-2}\,s^{-1}$)
W_J	RuBP-limited rate of carboxylation ($\mu mol\,m^{-2}\,s^{-1}$)

Greeks

α	apparent quantum yield of A at saturated CO_2 (mol CO_2 per mol photons)
β	angle of incidence (rad)
β^*	angle of the sun (rad)
β'	angle for scattered radiation (rad)

γ	psychrometric constant (Pa K^{-1})
δ	Boolean variable indicating whether leaves are hypo- or amphistomatous (–)
ε_c	phytoelement thermal emissivity (–)
λ	phytoelement angle (rad)
ξ	reflection–transmission distribution function (–)
ρ	density of dry air (kg m^{-3})
ρ_c	phytoelement reflection coefficient (–)
ρ_s	soil reflection coefficient (–)
σ	Stefan–Boltzmann constant ($5.67 \times 10^{-8}\,\text{W m}^{-2}\,\text{K}^{-4}$)
τ	RUBISCO specificity factor (–)
τ_c	phytoelement transmission coefficient (–)

Chen et al., 1999). Such models, given their reductionist nature, are of use if computational efficiency is given preference over numerical accuracy, as it is in meso-scale or global climate (GCM) model applications (Berry et al., 1998; Raupach et al., 1997; Cox et al., 1998; Anderson et al., 2000). A second line of models, often referred to as multi-layer models, retains the vertical profile of canopy structure and calculates micrometeorology and fluxes separately for each layer (e.g. Goudriaan, 1977; Tenhunen et al., 1994; Leuning et al., 1995; Baldocchi and Meyers, 1998; Tappeiner and Cernusca, 1998). These models represent useful tools for analysing the details of canopy CO_2 and energy exchange processes.

The overwhelming complexity of many natural and semi-natural canopies, though, places formidable practical problems, which has led to a variety of approaches, reflecting the respective scientific perspective. For example, many models consider the canopy to be composed solely of leaves, ignoring the existence of supporting structures (stems, twigs and branches), reproductive organs (inflorescences, fruits) and attached dead plant material (cf. Wenhan, 1993). This is manifested in the loose use of the term LAI (leaf area index), instead of PAI (plant area index), for the total above-ground silhouette area. Given the differing structural and functional properties of the various canopy components, it is clear that they contribute in different manners to whole canopy exchange processes. For example, dry dead plant material, as opposed to green matter, may dissipate absorbed energy solely via long-wave emission and sensible heat exchange (Paw U, 1987), and hence does not contribute to the canopy latent heat flux (Anderson

et al., 2000). In multi-species canopies, this issue becomes even more complicated, since within each of the various canopy components several species must be distinguished, which are likely to be characterised by different structural and functional properties (Tenhunen et al., 1994; Tappeiner and Cernusca, 1998; Sinoquet et al., 2000).

Semi-natural mountain grasslands fall both into the multi-component, as well as the multi-species category (Cernusca and Seeber, 1981; Tappeiner and Cernusca, 1994, 1995, 1996). These grasslands are often situated in the transition zone between the forest and the natural grasslands above the tree line, being created centuries ago by human activity (Spatz et al., 1978). The transitional character and sustainable management made them highly diverse ecosystems, populated by a large number of different plant species (Tasser et al., 1999). The various species follow different temporal strategies (Bahn et al., 1994), so that at almost any instant during the vegetation period we will find species at different stages of their life cycle, e.g. vigorous vegetative growth, flowering, fruiting, senescence. This strong variability also shows up in inter-specific differences with regard to gas exchange characteristics (Bahn et al., 1999; Wohlfahrt et al., 1999).

The aim of the present paper is to develop a model of vegetation–atmosphere CO_2 and energy exchange suitable for application to mountain grasslands, i.e. a model which allows for incorporating multiple canopy components and species. Concomitantly, a parameterisation strategy will be developed for the investigated canopies, and its plausibility assessed using a series of sensitivity tests. The parameterised model will be validated against independently measured data of bulk

canopy CO_2 and energy exchange. Finally, by considering the effects of simplifications in the input data likely to occur at larger spatial and/or temporal scales the applicability of the model at these larger scales will be assessed.

2. Materials and methods

2.1. Site

Field investigations were carried out within the frame of the EU-TERI-project ECOMONT during the summers of 1996–1998 in the Southern Alps on the Monte Bondone plateau (Trentino/Italy, latitude 46°01′20″N, longitude 11°02′30″E) at an elevation between 1500 and 1600 m above sea level. The mean annual temperature is 5.5°C ranging from −2.7°C in January to 14.4°C in July (Gandolfo and Sulli, 1993). Precipitation is abundant throughout the whole year (1189 mm), with two peaks in June (132 mm) and October (142 mm) and a minimum of 53 mm in January (Gandolfo and Sulli, 1993). Two sites, differing in land-use, were investigated: a hay meadow, mowed once a year, and an area abandoned 35 years ago. A

general characterisation of the two sites is given in Table 1 and in Cescatti et al. (1999).

2.2. Experimental methods

Leaf gas exchange measurements on the most abundant species (see below) were carried out as described previously in detail by Wohlfahrt et al. (1998, 1999) and are thus not repeated. A detailed description of the experimental set-up for measurements of microclimate and the fluxes of CO_2 and energy may be found in Tappeiner et al. (1999). Briefly, measurements were made using the battery-powered data acquisition system MIKROMET (Cernusca, 1987) at intervals ranging from 1 to 6 min, from which hourly mean values were calculated. Incoming short-wave radiation was measured using two star pyranometers, net radiation by the means of net radiometers (Schenk, Vienna, Austria). One star pyranometer was equipped with a shadow band in order to estimate the incoming diffuse solar radiation component. Soil temperatures (0, 0.05, 0.1, 0.2, and 0.5 m) and air temperatures within the canopy were measured using thermocouples (copper/constantan, 8×10^{-5} m diameter). Three-cup anemometers (Davis Instruments,

Table 1
General characterisation of the investigated sites at the Monte Bondone study area[a]

	Abandoned area	Meadow
Elevation (m a.s.l.)	1520	1520
Exposure	SE	E
Inclination (°)	6	3
Management	Abandoned for 35 years	Mowed
Vegetation type	Siversio-Nardetum strictae	Geranio-Trisetetum
Canopy height (m)	0.3	0.3
PAI ($m^2 m^{-2}$)[b]	4.7	4.2
LAI ($m^2 m^{-2}$)[b]	1.9	1.7
Mean phytoelement inclination angle (°)[b]	51	45
Soil type	Cambisol with mull	Cambisol with mull
Soil depth (m)	0.60	0.75
Rooting depth (m)[c]	0.20	0.20
Soil water storage capacity (m)[c]	0.31	0.34
Zero plane displacement (m)[d]	0.10	0.18
Momentum roughness parameter (m)[d]	0.023	0.049
log–exp wind profile intersection height (m)[d]	0.15	0.26
Wind speed extinction coefficient (–)[d]	2.71	2.91

[a] Data are from Cescatti et al. (1999), except for Footnotes b–d.
[b] Tappeiner and Sapinsky (unpublished).
[c] Neuwinger and Hofer (unpublished).
[d] Wohlfahrt et al. (2000).

Hayward, USA) were used to determine wind speed above the canopy. During calm conditions anemometers may stall and underestimate wind speed, which was accounted for by limiting wind speed above the canopy to a minimum value of $0.5\,\mathrm{m\,s^{-1}}$. CO_2 concentrations were measured using an infrared gas analyser (CIRAS-Sc, PP-Systems, Hitchin Herts, UK), water vapour pressure by the means of thermocouple psychrometers (Cernusca, 1991). The energy balance and the flux of CO_2 above the canopy were calculated by the Bowen-ratio-energy-balance (BREB) method. While we recognise that more advanced methods for measuring surface exchange processes exist (e.g. the eddy-covariance technique), preference was given to the simpler and cheaper BREB method, since it was our major goal to investigate a large number of different vegetation units. Positive flux densities represent mass and energy transfer directed away from the soil surface, negative values denote the reverse. Dry and wet-bulb temperatures, as well as CO_2 concentrations were measured at 0.1 and 0.7 m above the canopy, and 2 m above ground (Tappeiner et al., 1999). Soil heat flux (S) was estimated by a combination of the temperature integral method for the upper 0.2 m of the soil and the temperature gradient method for the lower layers of the soil (Tappeiner et al., 1999). CO_2 release from the soil (R_{soil}) was measured in situ by IRGA techniques as described by Cernusca and Decker (1989). Canopy net photosynthesis (A_C) was then calculated as $F_C + R_{soil}$, where F_C is the CO_2 flux above the canopy.

Canopy structure was assessed at the time of the biomass maximum (end of July) by stratified clipping (Monsi and Saeki, 1953) of a square plot of 0.3–0.5 m lateral length. Thickness of the harvested layers ranged between 0.02 and 0.04 m. Silhouette area was determined by the means of an area meter (LI-3100, Li-Cor, Lincoln, USA). The harvested plant material was separated as follows: leaves were separated into those having the largest fractional contribution to total PAI. Eight species were identified at the abandoned area (*Nardus stricta*, *Plantago atrata*, *Polygonum viviparum*, *Potentilla aurea*, *Ranunculus acris*, *Trifolium pratense*, *Trollius europaeus*, *Vaccinium myrtillus*) and nine at the meadow (*Alchemilla vulgaris*, *N. stricta*, *P. atrata*, *P. viviparum*, *P. aurea*, *R. acris*, *Rhinanthus alectorolophus*,

T. pratense, *T. europaeus*). In the following the first letter of the generic name followed by the full species names will be used to abbreviate species names, unless otherwise indicated. The remaining leaves were pooled to three functional groups: forbs, graminoids and dwarf shrubs (FL, GL and DL, respectively). Separation into these functional groups was also made for stems of forbs and graminoids (FS, GS); for dwarf shrubs further distinction was made between green (DgS) and non-green (DngS) woody stems. The remaining plant components, i.e. fruits (FRU), inflorescences (INF), attached dead plant material (NEC) and cryptogams (CRY), were pooled over all species. Altogether 17 components, as shown in Table 2, were distinguished at each site. In the following, these pooled quantities will be referred to as generic components. Phytoelement inclinations and widths were measured in the field with a hand inclinometer with a 5° accuracy and a ruler, respectively (Tappeiner and Sapinsky, 1999).

Table 2

Species and components (percentage of total PAI) distinguished within the canopies of an abandoned area and a meadow at the study area Monte Bondone[a]

Generic components	Abandoned area	Meadow
Fruits (FRU)	0.2	0.8
Inflorescences (INF)	0.2	1.1
Attached dead plant material (NEC)	55.4	50.2
Cryptogams (CRY)	–	0.3
Forb stems (FS)	1.7	3.0
Graminoid stems (GS)	1.5	5.0
Green dwarf shrub stems (DgS)	1.3	–
Non-green dwarf shrub stems (DngS)	0.8	–
Forb leaves (FL)	3.2	6.0
Graminoid leaves (GL)	17.3	20.3
Leaves separated into species		
A. vulgaris	–	0.1
N. stricta	1.9	1.2
P. atrata	6.5	2.7
P. viviparum	1.2	1.1
P. aurea	4.2	2.2
R. acris	0.3	0.2
R. alectorolophus	–	0.3
T. pratense	0.6	1.3
T. europaeus	1.3	4.2
V. myrtillus	2.4	–

[a] Abbreviations for the generic components are given in parenthesis.

2.3. Models

2.3.1. General aspects

In the present study, a one-dimensional, multi-layer model is used to compute the fluxes of CO_2, latent and sensible heat between the vegetation and the atmosphere. It consists of coupled micrometeorological and physiological modules. The micrometeorological modules compute radiative transfer (separately for the PPFD, near-infrared (NIR) and long-wave radiation (IR)) and the attenuation of wind speed. The profiles of CO_2, H_2O and air temperature within the canopy are not modelled, but instead, either measured values are used as input data or the profiles are kept constant (see below). The environmental variables computed in the micrometeorological modules represent the driving forces for the energy balance model, which partitions absorbed energy into emitted long-wave radiation, latent and sensible heat fluxes. Net photosynthesis, respiration, and stomatal conductance are calculated in a sub-module of the energy balance, whenever applicable (see below).

The phytoelements making up the canopy are separated into one of three physiological categories: A, B and C. Category A phytoelements are characterised by the ability to assimilate CO_2, such as leaves, green stems of herbaceous species and cryptogams. Category B covers the canopy components characterised by a positive CO_2 balance. All phytoelements with a positive CO_2 balance, including non-green, but also green woody stems of dwarf shrubs (Siegwolf, 1987), fit into this category. Finally, phytoelements classified as category C do not show any CO_2 gas exchange. Attached dead plant material is assigned to the last category, thereby neglecting CO_2 loss resulting from microbial decay. Besides CO_2 gas exchange, the three physiological categories also differ with respect to water vapour exchange: phytoelements classified as category A are capable of losing water via their stomata. Members of categories B and C are assumed to be non-transpiring (Anderson et al., 2000), which neglects peridermal transpiration by woody stems, as well as the loss of water absorbed by dead plant material.

Some of the following theory is kept short on purpose, since it was already topic of one of our previous papers, to which we refer for details. Symbols and abbreviations are given in Nomenclature.

2.3.2. Leaf gas exchange

Following theory developed by Farquhar and co-workers (Farquhar, 1979; Farquhar et al., 1980; Farquhar and Von Caemmerer, 1982), later modified according to Harley and Tenhunen (1991), CO_2 assimilation is either entirely limited by the kinetic properties of RUBISCO and the respective concentrations of the competing gases CO_2 and O_2 at the sites of carboxylation (W_C) or by electron transport (W_J), which limits the rate at which RuBP is regenerated. Limitations of RuBP regeneration arising from the availability of inorganic phosphate for photophosphorylation are not considered in the present approach. Net photosynthesis A may then be expressed as

$$A = \left(1 - \frac{0.5 O_i}{\tau C_i}\right) \min\{W_C, W_J\} - R_{day}, \qquad (1)$$

where O_i and C_i are the concentrations of O_2 and CO_2 in the intercellular space, respectively, τ is the specificity factor for RUBISCO (Jordan and Ogren, 1984), R_{day} the rate of CO_2 evolution from processes other than photorespiration and $\min\{\}$ denotes "the minimum of".

To be able to predict gas exchange at the leaf level, the photosynthesis model has to be combined with a model predicting stomatal conductance (Harley and Tenhunen, 1991). For this purpose the empirical model by Ball et al. (1987), modified according to Falge et al. (1996), was chosen

$$g_{sv} = g_{min} + 1000 G_{fac}(A + I_{fac} R_{dark}) \frac{h_s}{C_s}, \qquad (2)$$

where g_{sv} is the stomatal conductance, g_{min} the minimum or residual stomatal conductance and h_s and C_s are the relative humidity and the CO_2 concentration at the leaf surface. G_{fac} is an empirical coefficient representing the composite sensitivity of stomata to these factors. R_{dark} is the dark respiration and I_{fac} represents the extent to which dark respiration is inhibited in the light. Stomatal opening in response to PPFD is controlled via $(A + I_{fac} R_{dark})$, which gives an estimation of gross photosynthetic rate and is considered to be related to energy requirements for maintaining guard cell turgor (Falge et al., 1996).

Leaf internal CO_2 concentration is calculated from net photosynthesis and stomatal conductance

according to Fick's law:

$$C_i = C_s - \frac{1600A}{g_{sv}}, \qquad (3)$$

where 1600 accounts for the difference in diffusivity between CO_2 and H_2O (Farquhar and Sharkey, 1982) and the difference in the units of A and g_{sv}. Due to the fact that net photosynthesis and stomatal conductance are not independent, the model must solve for C_i in an iterative fashion (Harley and Tenhunen, 1991). Further details on the leaf gas exchange model may be found in Wohlfahrt et al. (1998).

2.3.3. Bole respiration

An Arrhenius-type equation is used to model respiration of woody stems as a function of temperature

$$R_{bole} = R_{bole}(T_{ref}) \exp\left[\frac{\Delta H_a}{R T_{ref}}\left(1 - \frac{T_{ref}}{T_{pK}}\right)\right], \qquad (4)$$

where $R_{bole}(T_{ref})$ is the respiration rate at the reference temperature (T_{ref}, 273.16 K), T_{pK} the absolute temperature, R the universal gas constant and ΔH_a an activation energy.

2.3.4. The energy balance

Phytoelement surface temperatures are estimated solving their energy balance equation (Campbell and Norman, 1998)

$$
\begin{aligned}
R_{abs} &= L_e + LE + H \\
&= 2\varepsilon_c \sigma T_{pK}^4 + \frac{\rho c_p}{\gamma}[e_s(T_p) - e_a]g_{tv} \\
&\quad + \rho c_p(T_p - T_a)0.924 g_{bv},
\end{aligned} \qquad (5)
$$

where R_{abs} is the bi-directional absorbed short-wave and long-wave radiation, L_e the emitted long-wave radiation, LE and H represent latent and sensible heat exchange, respectively, ε_c is the phytoelement thermal emissivity, σ the Stefan–Boltzmann constant, ρ and c_p are the density and the specific heat of dry air, respectively, γ is the psychrometric constant and g_{tv} the total conductance to water vapour. The calculation of g_{tv} depends on whether water is present on the phytoelement surfaces or not. In the absence of surface water, g_{tv} is calculated as

$$g_{tv} = \frac{g_{sv}g_{bv}\delta}{g_{sv} + g_{bv}\delta}, \qquad (6)$$

where g_{bv} is the all-sided boundary layer conductance to water vapour and δ is a Boolean variable indicating whether leaves have stomata on one ($\delta = 0.5$) or both ($\delta = 1$) leaf sides. Leaves and, due to the lack of appropriate data, green stems of the investigated species are treated as hypostomatous, although the latter might be supposed to have stomata distributed on the entire surface. Eq. (6) implies no latent heat exchange for dry phytoelements of categories B and C, since for these $g_{sv} = 0$. If phytoelements are wet (either due to dew formation, or the interception of precipitation or dew dripping down from upper canopy layers), g_{tv} reduces to g_{bv} (Nikolov et al., 1995). Dew forms on a phytoelement surface if the surface temperature drops below the dew point temperature of the surrounding air (Monteith, 1957). The calculations of dew dynamics recognise that phytoelements hold water up to a maximum capacity before the onset of dripping to the canopy components below, following an approach described by Wilson et al. (1999) and Anderson et al. (2000).

Boundary layer conductances to water vapour are modelled, following Nikolov et al. (1995), as the larger of the conductances resulting from forced and free convective exchange, making use of the non-dimensional groups (e.g. Monteith and Unsworth, 1990; Nobel, 1991). Characteristic phytoelement dimensions are taken as 0.7 width for leaves and dead attached plant material, approximating these as flat intersecting parabolas, and as the diameter for the remaining canopy components, approximating their shape as cylinders (Campbell and Norman, 1998). In order to account for the enhancement of boundary layer conductances due to the turbulent nature of outdoor environments a factor of 1.4 is included (Campbell and Norman, 1998). The boundary layer conductance to water vapour is converted to that for heat by the factor 0.924. The energy balance equation is solved in an analytical fashion following Nikolov et al. (1995), re-arranging it in a quartic form first proposed by Paw U (1987).

2.3.5. Within-canopy profiles of wind speed, CO_2 and H_2O concentration, and air temperature

A logarithmic equation is used to model wind speed in the sparse, upper canopy layers down to the upper height of the thick lower canopy layers (log–exp wind profile intersection height in Table 1), below

which attenuation proceeds exponentially (Wohlfahrt et al., 2000). A simple half-order closure scheme is adopted for the concentration profiles of CO_2 and H_2O, i.e. they are assumed to be constant within the canopy, which yields only small errors in the computation of CO_2 and latent heat fluxes (Baldocchi, 1992). Sensible heat exchange, on the other hand, depends strongly on the within-canopy air temperature profile (Baldocchi, 1992), which in the present approach is pre-described using measured profiles of within-canopy air temperature. Continuous profiles are generated by linear interpolation between air temperatures measured at different heights (usually seven). In the case that measured profiles of CO_2 and H_2O are available, the half-order closure assumption is abandoned and the same procedure as for air temperature is followed.

2.3.6. Radiative transfer

The model of radiative transfer treats the canopy as a horizontally homogeneous, plane-parallel turbid medium in which multiple scattering occurs on the elements of turbidity (phytoelements) of the different components, each having their own optical and geometrical properties. The canopy is divided into sufficiently small, statistically independent layers, within which self-shading may be considered negligible and phytoelements to be distributed symmetrically with respect to the azimuth. Hemispherical reflection and transmission of radiation, which are allowed to be unequal, are assumed to be lambertian. Nine inclination classes are considered. Details are given in Appendix A.

2.3.7. Numerical aspects

The present model involves five iteration loops: (i) two nested iterations in the gas exchange module in order to find a combination of A, C_i and g_{sv}, (ii) one iteration in order to find leaf temperatures compatible with the long-wave radiation profile (Wohlfahrt et al., 2000), and (iii) one iteration in finding the profiles of PPFD, NIR and IR. For the latter, a relaxation method, by which the scattered fluxes are added to the fluxes already there, is applied to solve for Eqs. (A.6), (A.9)–(A.13), as described in Goudriaan (1977). The corresponding convergence criteria were chosen as a compromise between numerical accuracy and computation time. For C_i and g_{sv} convergence criteria were

taken as $1\,\mu mol\,mol^{-1}$ and $1\,mmol\,m^{-2}\,s^{-1}$, respectively, for leaf temperatures as $0.1^{\circ}C$, and for radiation as $0.05\,W\,m^{-2}$. Tests with more stringent convergence criteria demonstrated that the aforementioned criteria are adequate.

Numerical stability and computation time of the above iterations also depend on their initialisation, i.e. on the choice of the starting values for the variables which are iterated for (except for (iii), where no starting values are employed; see above). In the first loop of the first time step, temperatures of sunlit and shaded phytoelements are initialised as air temperature $+3^{\circ}C$ and air temperature, respectively, C_i as $0.75C_a$ (Sage, 1994), and g_{sv} as 500 and $300\,mmol\,m^{-2}\,s^{-1}$ for sunlit and shaded phytoelements of category A, respectively. Since the gas exchange module is called every time phytoelement temperatures are up-dated, the values of C_i, g_{sv}, for category A, and equilibrium temperatures calculated during the previous loop are used as starting values in the following loops of the same time step. During subsequent time steps, the final values from the previous time steps are used.

The most time consuming iteration is the one for phytoelement equilibrium temperatures, due to the large number of calculations (including nested iterations in gas exchange module) involved. Using the above criteria, phytoelement temperatures usually converge within 3–6 loops. In the model of radiative transfer four loops are usually necessary to reach convergence in the NIR, three for the PPFD and IR. The model thus accounts for fourth-order scattering in the NIR waveband and for third-order scattering in the PPFD and IR wavebands.

2.3.8. Model testing

The model was extensively tested employing a budget approach: energy balance closure ($R_{Nveg} = LE + H$) was checked both at the organ and canopy level. Due to the fact that phytoelement temperatures are calculated by iteration, the energy balance is not completely closed, but the amount of residual energy is usually negligible, being less than 0.01 and $1\,W\,m^{-2}$ at the organ and canopy level, respectively. The model of radiative transfer was tested using an approach by Goudriaan (personal communication). Thereby sky, soil and phytoelements are assumed to be perfect black bodies (100% emission, no scattering) and at

the same absolute temperatures. Under these conditions long-wave radiation absorption and emission by phytoelements are equal, and hence R_{Nveg} is equal to zero. The discretisation into nine sky sectors gives rise to a small imbalance (Goudriaan, 1977), causing net radiation to deviate from the intended value, this deviation is though less than 0.5%. Consistency of the model of dew dynamics was checked by tracking the fate of water formed on phytoelements as dew. At the end of the simulation run, the total amount of dew formed during the run needs to be equal to the sum of dew evaporated into the atmosphere, dripped down to the soil surface and still present on the phytoelements. Using this approach, no imbalances were found using a wide range of meteorological forcing variables.

Model performance was assessed with respect to both quantitative and qualitative correspondence to measured data (cf. Pachepsky et al., 1996). Pearson's correlation coefficient and the F-test were used in order to test whether the model is quantitatively adequate. Qualitative model performance was evaluated by analysing deviations from 1:1 correspondence in the y-intercept and the slope obtained from linear regression analysis of observed versus predicted values.

3. Results and discussion

3.1. Parameterisation

3.1.1. Gas exchange

Parameterisation of the leaf gas exchange models of the investigated species was the topic of a previous paper (Wohlfahrt et al., 1998), and will therefore not be repeated. The corresponding parameters are shown in Table 3. The gas exchange parameters for the generic components, though, require some comments: Wohlfahrt et al. (1999) recently presented model parameters for the maximum rate of carboxylation (V_{Cmax}) and the potential rate of RuBP regeneration (P_{ml}) for 30 mountain grassland species, from which they derived generic model parameters for forbs, graminoids and dwarf shrubs, separately for meadows and abandoned areas. These parameters were adopted for leaves and stems of forbs and graminoids as shown in Table 4. Since *V. myrtillus* was by far the dominating dwarf shrub on the abandoned area, the

corresponding model parameters from Wohlfahrt et al. (1998) were used, instead of the generic dwarf shrub parameters from Wohlfahrt et al. (1999). Dark respiration parameters (unpublished, except for the species from the Monte Bondone study area, cf. Wohlfahrt et al., 1998) for these groups were calculated from the same data set. The apparent quantum yield of net photosynthesis at saturating CO_2 concentration, α (Harley and Tenhunen, 1991), was assigned an average value of 0.055 mol CO_2 mol per photon (Baldocchi and Meyers, 1998). Parameters of the stomatal conductance model (G_{fac} and g_{min}) must be considered site specific (Wohlfahrt et al., 1998) and were hence calculated, separately for the three functional groups, by averaging over the respective species from each site (Table 4).

Parameters describing bole respiration of green and non-green stems of dwarf shrubs were derived from gas exchange measurements on *Rhododendron ferrugineum* by Siegwolf (1987) and converted from a mass to an area basis using data by Gazarini (1988). In his studies Siegwolf (1987) found that respiration rates, in particular those of green stems, differed in light and darkness. This effect is accounted for by using two different parameter sets, both for green and non-green stems, depending on illumination, darkness being defined as PPFD $< 25\,\mu mol\,m^{-2}\,s^{-1}$ (Table 4).

3.1.2. Radiative transfer

In order to satisfy the criterion of negligible self-shading within the canopy layers, the PAI values measured at different heights in the canopies (Fig. 1) need to be further subdivided. The maximum PAI per layer, beyond which self-shading occurs, can be derived by considering the probability of non-interception, which is simply $(1 - P_i)$. The maximum PAI per layer, assuming a random phytoelement dispersion, is thus constrained by the phytoelement inclination distribution and the angle of incidence (cf. Eq. (A.1)). Taking a PAI of $0.1\,m^2\,m^{-2}$, which is considered as sufficient for this type of model by Goudriaan (1977), the minimum angle of incidence is around $3°$ for a spherical phytoelement inclination distribution. This seems tolerable, since (i) direct radiation is small at such grazing angles and (ii) this is less than the median of the lowest sky sector ($5°$) considered for the attenuation of diffuse radiation. A layer size of $0.1\,m^2\,m^{-2}$ PAI is hence used.

Table 3

Parameters of the combined leaf photosynthesis (A) and stomatal conductance (B) model for the investigated key-species: A. *vulgaris* (Alvu), *N. stricta* (Nast), *P. atrata* (Plat), *P. viviparum* (Povi), *P. aurea* (Poau), *R. acris* (Raac), *R. alectorolophus* (Rhal), lower (lo) and upper (up) leaves of *T. europaeus* (Treu), *T. pratense* (Trpr) and *V. myrtillus* (Vamy)[a]

Parameter	Units	Site	Alvu	Nast	Plat	Povi	Poau	Raac	Rhal	Treu$_{lo}$	Treu$_{up}$	Trpr	Vamy
(A) *Photosynthesis model*													
V_{Cmax}													
$V_{cmax}(T_{ref})$	μmol m^{-2} s^{-1}		64.17[b]	37.93	52.88	37.16	30.03	80.79[b]	53.24	35.07	18.89	48.79	13.30
$\Delta H_a(V_{Cmax})$	J mol^{-1}		105945[b]	61304	64490	60940	57098	98400[b]	60600	68000	68362	53017	102568
$\Delta H_d(V_{Cmax})$	J mol^{-1}		197250[b]	202583	200000	199571	204000	196900[b]	202000	201000	202198	202000	201194
P_{ml}													
$P_{ml}(T_{ref})$	μmol m^{-2} s^{-1}		28.50[b]	25.29	31.18	27.85	17.48	49.81[b]	26.71	22.93	11.97	27.03	5.57
$\Delta H_a(P_{ml})$	J mol^{-1}		56324[b]	44386	51014	61521	57101	66000[b]	37407	55465	55465	68707	57329
$\Delta H_d(P_{ml})$	J mol^{-1}		198582[b]	196168	197551	192521	199247	194000[b]	201000	199521	199521	199000	198922
R_{dark}													
$R_{dark}(T_{ref})$	μmol m^{-2} s^{-1}		1.08[c]	2.02	1.58	2.68	0.68	2.16[c]	1.47	1.24	1.01	0.80	1.31
$\Delta H_a(R_{dark})$	J mol^{-1}		53460[c]	13592	53132	17913	94482	58053[c]	70418	36743	37246	40479	22821
α	mol CO$_2$ per mol photons		0.06[c]	0.05	0.05	0.06	0.06	0.065[c]	0.06	0.06	0.045	0.06	0.06
(B) *Stomatal conductance model*													
G_{fac}	–	A	–	16.0	9.8	12.0	24.7	7.6[c]	–	12.8	20.2	6.9	10.5
		M	7.0[c]	16.0	13.8	11.9	17.0	7.6[c]	18.3	13.4	19.2	6.9	–
g_{min}	mmol m^{-2} s^{-1}	A	–	21.9	76.1	54.5	130.0	124.4[c]	–	70.6	94.7	25.2	11.7
		M	80.8[c]	21.9	70.0	57.0	120.0	124.4[c]	193.1	67.0	29.5	25.2	–

[a] For abbreviations and symbols, see Nomenclature (A: abandoned area, M: meadow). $\Delta S(V_{Cmax})$ and $\Delta S(P_{ml})$ were fixed for all species at 656 and 643 J K^{-1} mol^{-1}, respectively (cf. Wohlfahrt et al., 1998). Parameters are from Wohlfahrt et al. (1998), except for Footnotes b and c.

[b] Wohlfahrt et al. (1999).

[c] Wohlfahrt et al. (unpublished data).

Table 4
Parameters of (A) the combined photosynthesis and stomatal conductance model for leaves and stems of forbs (FL and FS, respectively), graminoids (GL and GS, respectively) and cryptogams (CRY), and (B) of the bole respiration model for green (DgS) and non-green (DngS) stems of dwarf shrubs[a]

Parameter	Units	Meadow		Abandoned area			
		FL, FS, CRY	GL, GS	FL, FS	GL, GS	DgS	DngS
(A) *Combined photosynthesis and stomatal conductance model*							
V_{Cmax}							
$V_{cmax}(T_{ref})$	$\mu mol\,m^{-2}\,s^{-1}$	53.52	39.41	35.86	36.24		
$\Delta H_a(V_{Cmax})$	$J\,mol^{-1}$	69752	87624	69022	55125		
$\Delta H_d(V_{Cmax})$	$J\,mol^{-1}$	200652	198801	200336	201578		
P_{ml}							
$P_{ml}(T_{ref})$	$\mu mol\,m^{-2}\,s^{-1}$	28.73	22.21	21.21	23.66		
$\Delta H_a(P_{ml})$	$J\,mol^{-1}$	48840	75926	52710	46270		
$\Delta H_d(P_{ml})$	$J\,mol^{-1}$	198190	194482	197095	196019		
R_{dark}[b]							
$R_{dark}(T_{ref})$	$\mu mol\,m^{-2}\,s^{-1}$	1.52	0.94	1.56	1.46		
$\Delta H_a(R_{dark})$	$J\,mol^{-1}$	48966	93544	51628	49942		
α[c]	$mol\,CO_2$ mol per photons	0.055	0.055	0.055	0.055		
G_{fac}[b]	–	14.4	15.4	15.9	16.0		
g_{min}[b]	$mmol\,m^{-2}\,s^{-1}$	80.3	75.8	85.2	21.9		
(B) *Bole respiration model*							
R_{dark}[d]							
$R_{dark}(T_{ref})$	$\mu mol\,m^{-2}\,s^{-1}$					3.04	1.17
$\Delta H_a(R_{dark})$	$J\,mol^{-1}$					53807	46834
R_{day}[d]							
$R_{day}(T_{ref})$	$\mu mol\,m^{-2}\,s^{-1}$					0.60	0.34
$\Delta H_a(R_{day})$	$J\,mol^{-1}$					117432	104467

[a] For abbreviations and symbols, see Nomenclature. $\Delta S(V_{Cmax})$ and $\Delta S(P_{ml})$ were fixed for all components of (A) at 656 and 643 $J\,K^{-1}\,mol^{-1}$, respectively (cf. Wohlfahrt et al., 1998). Parameters are from Wohlfahrt et al. (1999), except for Footnotes b–d.
[b] Wohlfahrt et al. (unpublished).
[c] Baldocchi and Meyers (1998).
[d] Siegwolf (1987).

Phytoelement inclination distributions, as well as widths, of the generic components were found as averages over the species for which detailed measurements were made, weighted by their PAI.

The model of radiative transfer assumes a random distribution of phytoelements (Goudriaan, 1977). Clumping occurs if phytoelements are grouped together, so that more radiation penetrates as compared to a random distribution; the reverse is true for a regular distribution, where phytoelements tend to avoid each other's presence (Baldocchi and Collineau, 1994). Assuming a random phytoelement distribution in a simpler version of the present model, Wohlfahrt et al. (2000) found reasonable correspondence be-tween modelled and measured within-canopy profiles of PPFD. Using the present, more elaborate model version together with the same data set as Wohlfahrt et al. (2000), model predictions match observed values even closer (data not shown). The assumption of a random phytoelement distribution is hence kept.

Vegetation and soil optical properties, lacking own measurements, were borrowed from various literature sources, as detailed in Table 5. Fruits, inflorescences and cryptogams, due to the lack of an appropriate literature source, were assigned parameters for green leaves from Asner et al. (1998a). For stems of herbaceous species and green stems of dwarf shrubs the same parameters as for their leaves were used. Soil
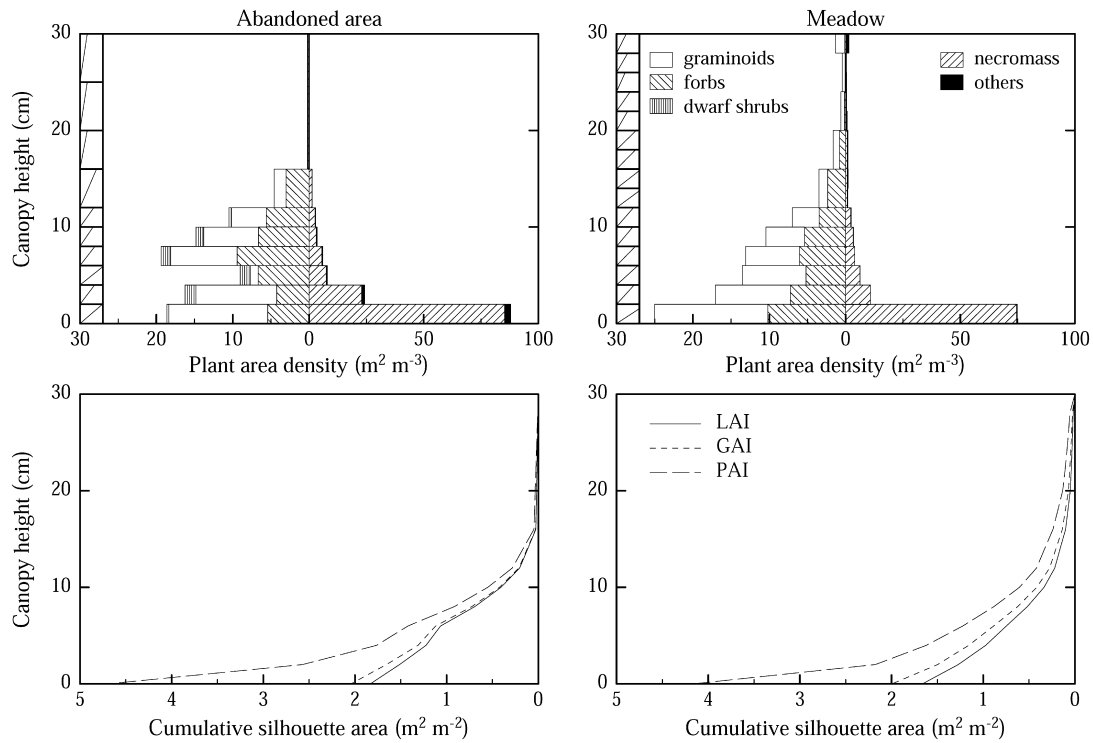
Fig. 1. Vertical canopy structure for an abandoned area and a meadow at the study area Monte Bondone. Photosynthetically active and non-active canopy components are drawn to left and the right of the figures in the upper panel, respectively. Average phytoelement inclination angles are indicated to the left of the figures in the upper panel. The lower panels show the cumulative LAI, green area index (GAI) and PAI.

Table 5
Vegetation and soil optical properties for the wavebands of PPFD, NIR and IR (for abbreviations, see Nomenclature)

	PPFD		NIR		IR reflection
	Reflection	Transmission	Reflection	Transmission	
FL, FS, GL, Gs[a]	0.12	0.06	0.38	0.37	0.04[b]
FRU, INF, CRY[a]	0.12	0.06	0.38	0.37	0.04[b]
DL, DgS[a]	0.09	0.06	0.43	0.39	0.04[b]
DngS[c]	0.15	–	0.35	–	0.04[b]
NEC[a]	0.42	0.13	0.53	0.21	0.04[b]
Soil	0.15[d]	–	0.25[e]	–	0.07[f]

[a] Asner et al. (1998a).
[b] Nobel (1991).
[c] Asner et al. (1998b).
[d] Asner and Wessman (1997).
[e] Goudriaan (1977).
[f] Monteith (1977).

reflectance is influenced in a complex fashion by several factors, such as water content (e.g. Jacquemoud et al., 1992) and soil physical and chemical properties (e.g. Baumgardner et al., 1985). Parameters have been thus chosen such that they fall into the middle of the range described in literature for each of the three wavebands (Table 5).

3.2. Sensitivity analysis

In order to asses potential deviations in model predictions introduced by selecting inappropriate parameter values, a sensitivity analysis was conducted varying, within a reasonable range, the parameters for which no measured values were available. This concerns vegetation and soil optical properties, dwarf shrub bole respiration parameters, and inclination distribution, width and physiology of the generic components. Simulations were conducted for two contrasting weather scenarios, a clear and an overcast day, respectively, using meteorological forcing variables as they are typically encountered at the study area at the end of July (Table 6). The same meteorological variables were used for both canopies, thus neglecting potential feedback effects by canopy processes on these variables.

3.2.1. Optical properties

Soil and vegetation optical properties determine the amount of absorbed, emitted (long-wave only) and scattered radiation, the latter two being made available for interaction with other objects. Increases in soil reflectance result in radiation formerly absorbed by the soil, i.e. energy "lost" to the vegetation, be-

ing redirected into the canopy (Asner and Wessman, 1997). Part of this upward radiation flux is absorbed, increasing R_{Nveg}, the vegetation net radiation, which in turn causes phytoelement temperatures to rise as indicated by an increase in H (Fig. 2). Higher leaf temperatures in turn stimulate LE (Fig. 2) by increasing the air-to-leaf-vapour-pressure-difference (ALVPD). A_C profits from the additional availability of scattered PPFD. Quantitatively the effects are though almost negligible, being less than 1% for alterations in soil optical properties of 30% (Fig. 2). Increasing phytoelement scattering coefficients leads to a decrease in radiation absorption at the phytoelement level and ultimately to increased radiation loss from the canopy (Asner and Wessman, 1997). The decreased net radiation causes phytoelement temperatures to decline, as indicated by the decrease of H and LE (Fig. 2). The decrease in LE is though fairly small, due to the fact that decreased leaf temperatures cause A_C slightly to increase (Fig. 2), which through Eq. (2) in turn increases g_{sv} and hence ultimately LE. Decreased phytoelement temperatures cause the emission of long-wave radiation by the phytoelements to decrease and hence increase R_{Nveg}, this effect is though offset by an increase of the reflected radiation component (Fig. 2). Alterations of the vegetation optical properties are quantitatively much more important as compared to those of the soil, e.g. increasing the phytoelement scattering coefficients by 30% results in a decrease in H by up to 90%. Differences between the abandoned area and the meadow, as well as with regard to clear and overcast weather situations, are generally small, both for soil and vegetation optical properties.

3.2.2. Dwarf shrub bole respiration

Altering the respiration rate of green and non-green stems of dwarf shrubs affects canopy carbon gain of the abandoned area only slightly, as shown in Fig. 3. This is not surprising, given the small contribution to the total PAI of 2.1% (Table 2).

3.2.3. Structural and functional properties of the generic components

Generic components assigned to physiological category A (FL, GL, FS, GS and CRY) make up 23.7 and 34.6% of the total PAI of the abandoned area and the meadow, respectively (Table 2). Physiological

Table 6
Meteorological forcing variables employed in sensitivity analysis[a]

Parameter	Clear day		Overcast day	
	Minimum	Maximum	Minimum	Maximum
T_a (°C)	8.5	19.0	11.5	17.4
e_a (hPa)	10.7	15.5	12.3	15.9
T_s (°C)	10.4	20.8	11.2	18.9
Q_{solar} (W m^{-2})	0	830	0	180

[a] Clear and overcast day scenarios refer to typical weather situations at the study area during the end of July. CO_2 concentration and wind speed above the canopy were kept constant at $350 \mu mol\, mol^{-1}$ and $2\, m\, s^{-1}$, respectively. For abbreviations, see Nomenclature.
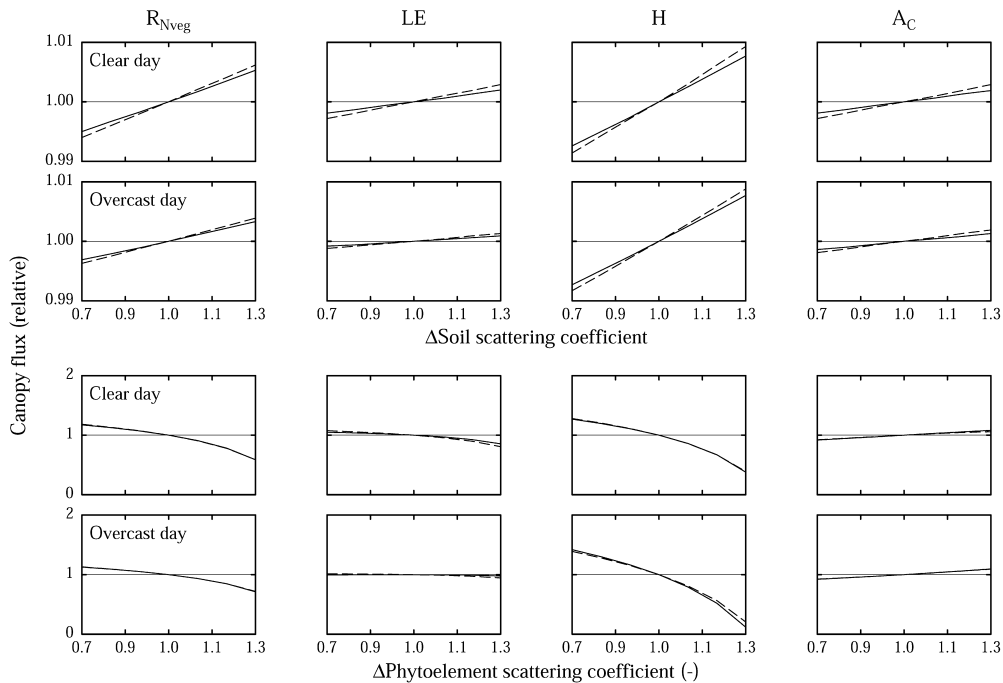
Fig. 2. Sensitivity analysis investigating the effects of altered soil and vegetation optical properties on daily sums (sun rise till sun set) of vegetation net radiation (R_{Nveg}), latent (LE) and sensible (H) heat exchange, and canopy net photosynthesis (A_C) of an abandoned area (solid lines) and a meadow (dashed lines) at the study area Monte Bondone. Exchange rates are expressed relative to those obtained using the original parameters. Note the different scales on the y-axis.

parameters for these components were found by averaging, as described above and in Wohlfahrt et al. (1999). The sensitivity of bulk canopy exchange rates to these parameters was assessed as shown in Fig. 4. The photosynthetic potential was altered by varying the maximum rate of carboxylation (V_{Cmax}), and by scaling the potential rate of RuBP regeneration (P_{ml}) and the dark respiration rate (R_{dark}) in proportion to V_{Cmax}. According to the model of Wohlfahrt et al. (1998) this procedure is equivalent to altering the nitrogen content. Increasing V_{Cmax} leads to an increase in A_C, accompanied by an increase in LE due to the dependence of g_{sv} on A as expressed in Eq. (2). Since no additional energy is available to the system, R_{Nveg} is virtually constant and H decreases accordingly. Stomatal conductance was altered by varying G_{fac}, a coefficient which determines the correlation between net photosynthesis and stomatal conductance (Ball et al., 1987). Increasing G_{fac} leads to an increase of g_{sv} and hence LE, which, in terms of available energy,

is compensated by a decrease in H. Higher stomatal conductances allow for more CO_2 to enter the leaves, increasing C_i and in turn A_C. Differences between clear and overcast day scenarios are generally small, effects being slightly more pronounced during clear days. Carbon gain of the meadow is slightly more sensitive to alterations of photosynthetic parameters as compared to the abandoned area (Fig. 4). This is mainly due to the fact that at the meadow the generic components make up a larger portion of the total biomass as compared to the abandoned area. In fact, if put to a PAI basis, it turns out that the generic components of the abandoned area would be more efficient in using additional photosynthetic potential.

Further simulations aiming at testing the sensitivity of bulk canopy predictions of R_{Nveg}, LE, H and A_C to alterations ($\pm 30\%$) of the inclination distribution and width of the generic components, showed a minor sensitivity in the case of the phytoelement inclination distribution ($<5\%$ effect), and even less ($<3\%$
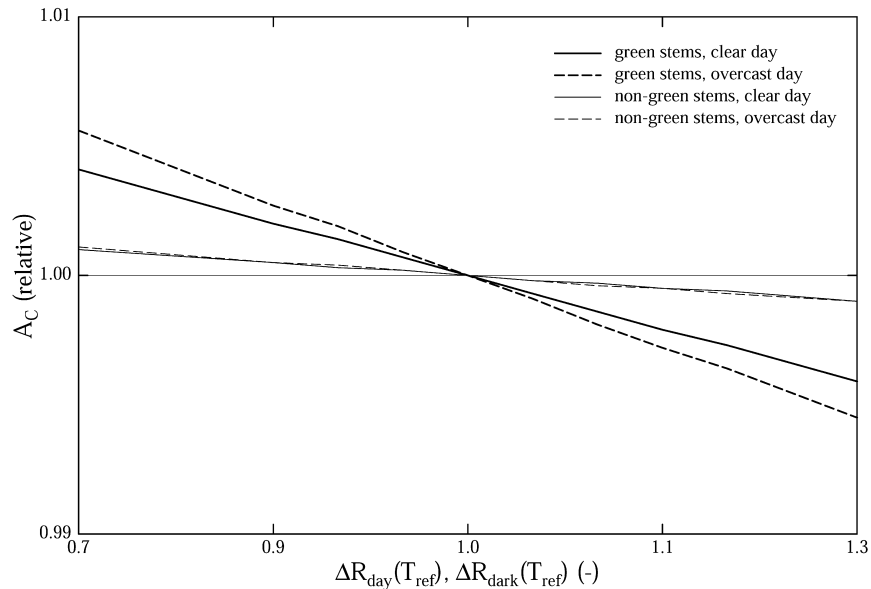
Fig. 3. Sensitivity analysis investigating the effects of altered respiration rates of green and non-green dwarf shrub stems on the daily sum (sun rise till sun set) of canopy net photosynthesis (A_C) of an abandoned area at the study area Monte Bondone. Exchange rates are expressed relative to those obtained using the original parameters.

effect) sensitivity for phytoelement widths (data not shown).

3.3. Validation

The ability of the multi-component vegetation–atmosphere-transfer (VAT) model to adequately simulate the exchange of CO_2 and energy between the vegetation and the atmosphere is assessed by comparing model predictions with independent above-canopy measurements of CO_2 and energy exchange.

The net radiation balance of the canopy (R_N) must be simulated accurately, if we are to compute realistic latent and sensible heat and CO_2 flux densities (Baldocchi and Harley, 1995). A comparison between observed and predicted net radiation flux densities (Fig. 5) reveals, that the model is fairly well capable of simulating low values of R_N, but increasingly underestimates high values, as also indicated by the linear regression analysis in Table 7. During clear days around noon, the upwelling radiation flux density is overestimated by up to $60 \, W \, m^{-2}$, which is about twice the value quoted as the typical accuracy of net radiation measurements (Halldin and Lin-

droth, 1992; Smith et al., 1997). Since reflection of long-wave radiation represents only a small fraction of the upwelling radiation flux (Campbell and Norman, 1998), this indicates that either simulated leaf temperatures, and hence the long-wave emission, or reflected short-wave radiation (i.e. the albedo), are too high. Comparing measured and predicted albedo (data available only for meadow) reveals, that the albedo is slightly underestimated (around 5%), probably due to phytoelement scattering coefficients being too low in the short-wave (cf. Fig. 2). This would suggest erroneously high leaf temperatures to be the reason for the observed overestimation of the upwelling radiation flux. A comparison of measured and simulated leaf temperatures (data not shown) indeed indicates an overestimation of up to 2–3°C. Yet, simulations with artificially lowered leaf temperatures, indicate that an overestimation of this magnitude cannot account for the increased long-wave emission. Possibly, also deviations from a random phytoelement distribution may be the cause for the observed discrepancy. Results in this vein have been obtained by Baldocchi and Harley (1995), who found R_N to be underestimated in a deciduous forest if clumping of phytoelements was not
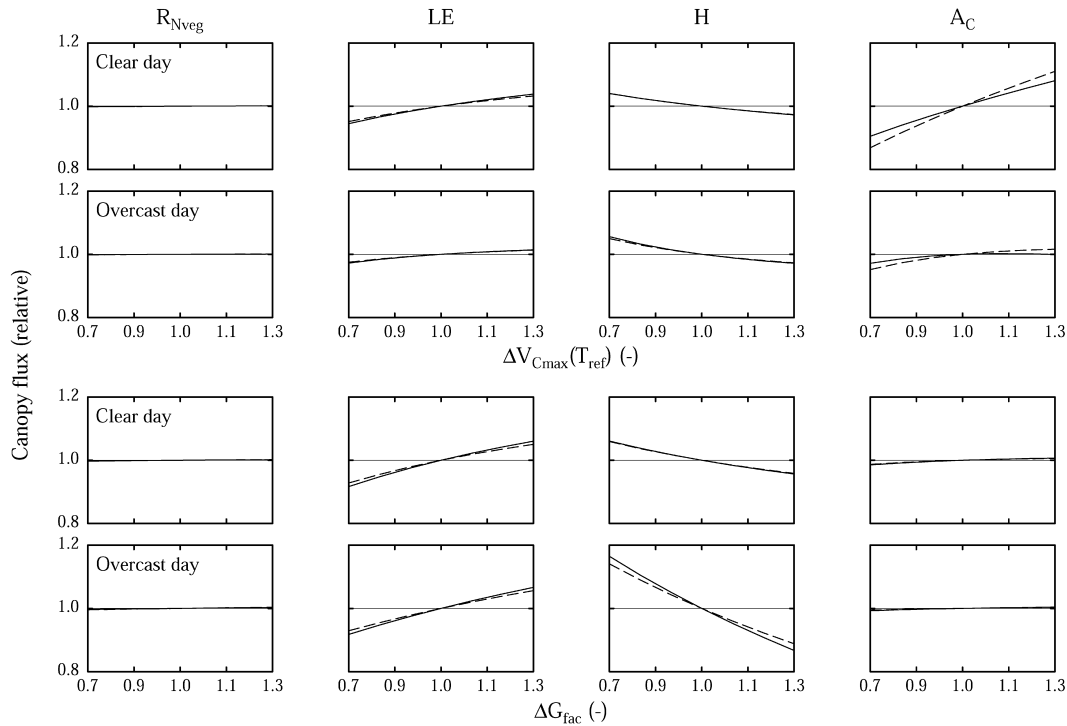
Fig. 4. Sensitivity analysis investigating the effects of altered leaf gas exchange model parameters of the generic groups on the daily sums (sun rise till sun set) of vegetation net radiation (R_{Nveg}), latent (LE) and sensible (H) heat exchange, and canopy net photosynthesis (A_C) of an abandoned area (solid lines) and a meadow (dashed lines) at the study area Monte Bondone. Exchange rates are expressed relative to those obtained using the original parameters.

accounted for. For forest ecosystems it should, how-ever, be noted, that the upwelling radiation may show considerable spatial variation due to the heterogeneity of the underlying soil–vegetation surface. Droppo and Hamilton (1973) report a 13% difference in net radi-ation above a deciduous forest when measured simul-taneously from towers 15 m apart, and Anthoni et al. (1999) found upwelling radiation to vary spatially by $60 \, W \, m^{-2}$ above an open-canopied ponderosa pine forest. For the grasslands under study the spatial variation in R_N remains yet to be determined. We conclude that a combination of the effects of the het-erogeneity of the underlying soil–vegetation surface, measurement accuracy, and a small systematic over-estimation of phytoelement temperatures is likely to be the main reason for the observed underestimation of R_N.

Validating canopy latent and sensible heat exchange proves somewhat problematic, since the correspond-ing measurements by the BREB method include soil latent and sensible heat exchange, which the present VAT model does not account for. Soil evaporation under closed vegetation is generally estimated to comprise 10–20% of total evapotranspiration (Rutter, 1979), a systematic underestimation of the measured LE flux by this magnitude may thus be expected from model predictions. Indeed, a linear regression analysis (Table 7) of observed versus predicted LE values (Fig. 5) reveals a small bias towards lower val-ues. The average underestimation is about 5% for the abandoned area and 10% for the meadow, the latter thus approaching the lower limit of the range reported by Rutter (1979). Overestimation of canopy LE might be due to the fact, that in the present modelling ap-proach the within-canopy water vapour pressures are kept constant at the above-canopy values. Within the canopy, water vapour pressures are usually enhanced with respect to the values above the canopy, due to
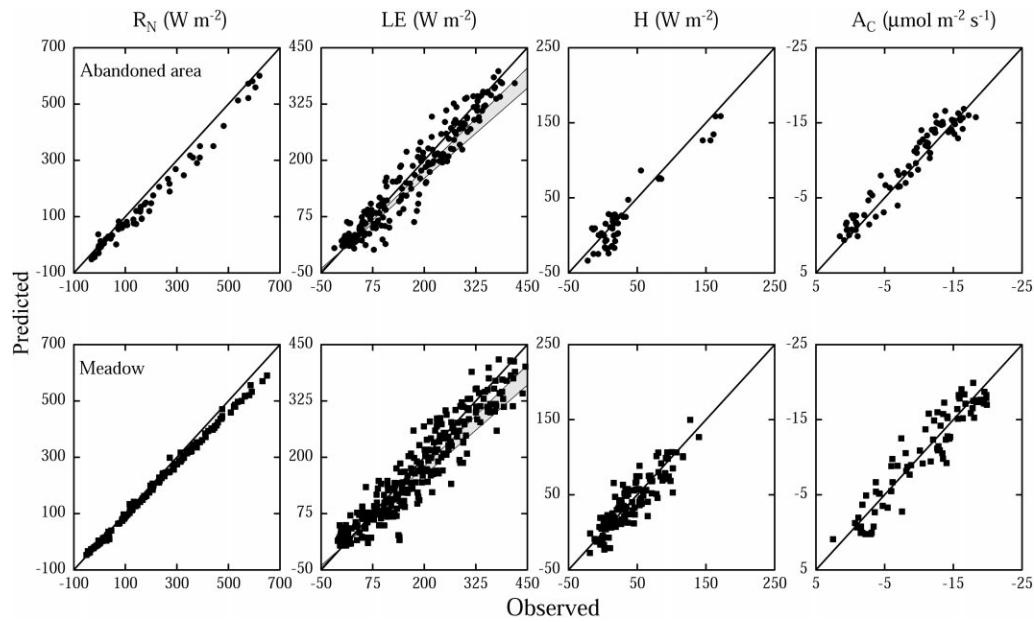
Fig. 5. Comparison of observed versus predicted values of net radiation (R_N), latent (LE) and sensible (H) heat exchange, and canopy net photosynthesis (A_C) of an abandoned area and a meadow at the study area Monte Bondone. Solid lines indicate 1:1 correspondence. The two lines below the 1:1 line on the LE plot indicate estimated 1:1 correspondence for pure canopy evapotranspiration, assuming a 10 and 20% reduction by soil evaporation (Rutter, 1979).

water vapour released by soil and vegetation (Finnigan and Raupach, 1987). Using water vapour pressures from above the canopy thus artificially increases the ALVPD, and ultimately transpiration (given stomatal conductance remains constant). The resulting error in the computation of whole canopy LE may though supposed to be small, as demonstrated in a simulation study for a soybean canopy by Baldocchi (1992). Quantifying the contribution of the soil to the total sensible heat flux proves even more difficult, since no simple rule-of-thumb, as for soil evaporation, exits. This is mainly due to the fact that both magnitude

Table 7
Results of a linear regression analysis of observed versus predicted values of net radiation (R_N) and the fluxes of latent (LE) and sensible (H) heat, as well as net photosynthesis (A_C)[a]

Parameter	Site	Slope	y-Intercept	r	F	$F_{crit.}$
R_N	A	0.94 ± 0.02	-19.75 ± 4.04	0.99	3409.12	7.04
	M	0.92 ± 0.01	-0.58 ± 1.24	0.99	46826.80	6.84
LE	A	0.95 ± 0.02	1.18 ± 3.77	0.96	2576.90	6.76
	M	0.89 ± 0.02	8.52 ± 3.49	0.95	2817.87	6.72
H	A	0.92 ± 0.05	-3.08 ± 2.73	0.95	387.88	7.22
	M	0.90 ± 0.04	3.09 ± 2.08	0.89	496.46	6.84
A_C	A	0.94 ± 0.03	1.20 ± 0.29	0.97	1070.57	6.96
	M	0.96 ± 0.04	0.26 ± 0.50	0.94	569.96	6.96

[a] Model performance is evaluated by the slope and the y-intercept of a regression line through observed versus predicted values (mean $\pm$ standard error), Pearson's correlation coefficient (r) and by comparison of the F-value (F) with the critical F-value ($F_{crit.}$, F-value at $p = 0.01$) (A: abandoned area, M: meadow).

and direction of the soil sensible heat flux are fairly variable (e.g. Raupach et al., 1997). Its sign depends on whether soil surface temperatures are above or below that of the adjacent air layer, whereas soil evaporation remains positive even if soil surface temperatures are below air temperature as long as the water vapour gradient is positive (Campbell, 1985). Soil surface temperatures (data not shown) are generally above that of the adjacent air layer at the meadow (a positive sensible heat flux), whereas a distinct diurnal pattern is observed at the abandoned area. There, the soil surface, as compared to the adjacent air layer, heats up more quickly during the morning, the soil sensible heat flux being positive until the early afternoon, when soil surface temperature drops below air temperature, the sensible heat flux then being negative until the morning. The model thus should underestimate measured H at the meadow, whereas both over- and underestimation should occur at the abandoned area. Yet, as shown in Table 7, H is slightly underestimated at both sites. Since H is fairly sensitive to the profile of within-canopy air temperature (Baldocchi, 1992), this discrepancy may be due to errors associated with unattended measurements of within-canopy air temperatures, which are somewhat tricky in such dense canopies. Plant parts moved by the wind easily displace the thermocouples from the intended positions exposing them to solar radiation or causing contact with neighbouring canopy elements or supporting experimental structures. Clearly, further experiments, aiming at separating vegetation and soil energy fluxes, are needed to satisfactorily validate the present model.

As shown in Fig. 5, the model is well capable of predicting canopy net photosynthesis, the slopes and y-intercepts being close to 1 and 0, respectively, as well as the F-values exceeding the critical ones (Table 7). At the abandoned area, though, the residuals indicate a slight qualitative deficiency, a larger fraction of measured values being overestimated (Fig. 5). This is likely to be caused by the spatial heterogeneity within the fetch of the BREB measuring system. Parts of the abandoned area are composed by stands dominated by dwarf shrubs (mainly *V. myrtillus*), which are characterised by smaller carbon gains as compared to the investigated canopy. This is due to their smaller leaf photosynthetic potential (Cernusca et al., 1992; Bahn et al., 1999; Wohlfahrt et al., 1999), as well as their unfavourable ratio between photosynthetically active and non-active biomass (Tappeiner and Cernusca, 1996, 1998; see also Fig. 1 and Tables 1 and 2). During periods when the wind conveys air parcels originating from dwarf shrub dominated parts of the abandoned area past the sensors of the measuring system, overestimation by the model occurs. Similar problems have been encountered in several other modelling studies (e.g. Williams et al., 1996). These data could be removed from the validation data set by excluding the sectors where such contamination is likely to occur, this was though not done in the present case, given the minor nature of the resulting deviations.

3.4. Model application

In the present approach, modelling is taken to a very detailed level, explicitly considering the different structural and functional characteristics of the various vegetation components. The price for this high level of detail, inevitably, is a large number of input parameters, which clearly represents a drawback for application of the present modelling approach at larger spatial and/or temporal scales for which such detailed data will hardly be available (Running et al., 1999). In the following, we hence employ the present model in order to test for the quantitative effects of some simplifying assumptions, which may need to be made if one aims at predictions at larger spatial and/or temporal scales.

Many models of radiative transfer consider the phytoelement inclination distribution to be (i) independent of height and to be (ii) well represented by some predefined distribution (e.g. Goudriaan, 1977; Leuning et al., 1995). The most popular among the predefined inclination distributions is probably the spherical one ($\approx 57°$ average angle), which has been found to be suitable for many crops (e.g. maize: Goudriaan, 1977; soybean: Baldocchi, 1993), because it considerably simplifies computation of radiative transfer, O_{av} being equal to 0.5 independent of the angle of incidence (De Wit, 1965). Assuming a spherical phytoelement distribution for the two investigated canopies causes only marginal changes (maximum deviation <5%) in the resulting bulk canopy predictions (Fig. 6–I). This is due to the fact, that the largest deviations with respect to real phytoelement angles (Fig. 1) occur in the upper- and lowermost canopy layers. These areas contribute only a small fraction to the whole canopy
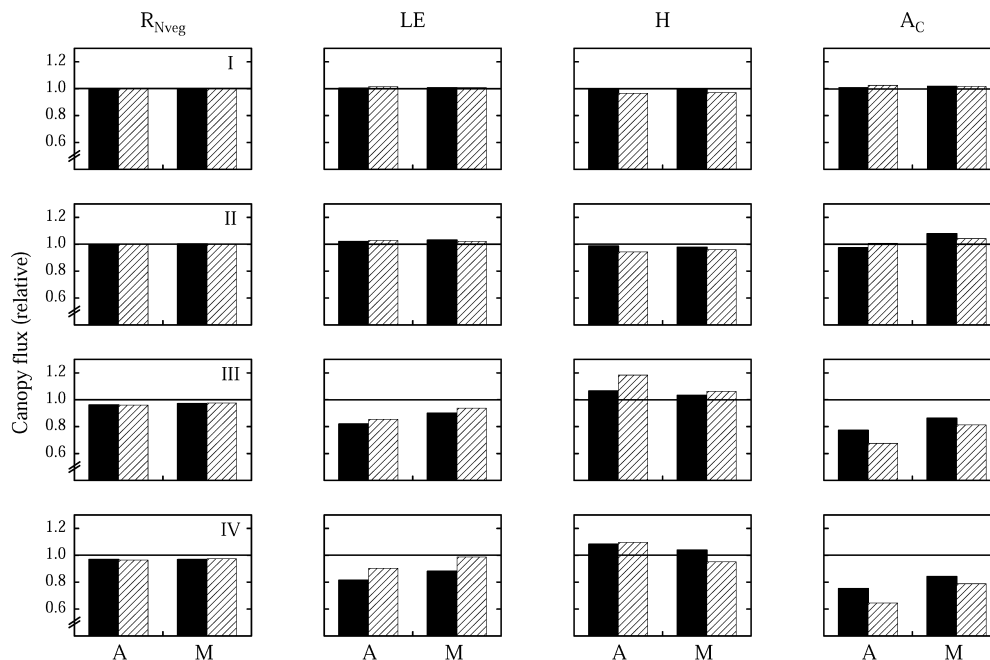
Fig. 6. Sensitivity analysis investigating the effects of assuming (I) a spherical phytoelement angle distribution, (II) species physiology to be represented by three functional groups, and a homogeneous vertical phytoelement distribution in the canopy as a whole (III) and separately in an upper and lower layer (IV), on vegetation net radiation (R_{Nveg}), latent (LE) and sensible (H) heat exchange, and canopy net photosynthesis (A_C) for an abandoned area (A) and a meadow (M) at the study area Monte Bondone. Daily sums (sun rise till sun set) of exchange rates are expressed relative to those obtained using the original parameters. Black bars indicate clear, hatched bars overcast weather conditions.

fluxes — the former because of the small amount of phytoelement area (Fig. 1), the latter because of the prevailing unfavourable environmental conditions, mainly the reduced light availability.

When dealing with the gas exchange of multi-species vegetation communities some simplifications regarding the description of leaf physiology need to be made. Up to this point we followed a mixed approach, using species-specific parameters for the key-species, whereas the remaining species were categorised into three functional groups and assigned respective generic values (see above). In the following the concept of functional groups (cf. Dawson and Chapin, 1993; Chapin, 1993) will be extended to the photosynthetically active phytoelements of all species, i.e. with regard to leaf gas exchange only forbs, graminoids and dwarf shrubs will be distinguished (for parameters refer to Table 4). As shown in Fig. 6–II, such a reduction of physiological input

parameters, keeping all other parameters constant, affects bulk canopy processes by less than 6%. This example clearly shows the potential of using the concept of functional groups for aggregating leaf physiological parameters, given of course a representative data basis exists. Recently, much effort in compiling corresponding data sets has been undertaken (e.g. Wullschleger, 1993; Reich et al., 1998a,b; Niinemets, 1999; Medlyn et al., 1999; Wohlfahrt et al., 1999), so that similar approaches should become feasible in the near future also for other ecosystems.

Despite the increasing number of vegetation-related products derived from remote sensing applications (e.g. aircraft or satellite observations; cf. Running et al., 1999), a large-scale determination of the detailed vertical canopy structure remains elusive, and it is hence instructive to explore the sensitivity of the model to corresponding simplifications in the input data. In a first scenario, the results of which are shown

in Fig. 6–IV, we hence assumed the total PAI, but not the vertical distribution of phytoelements, to be available as input data. In a second scenario (Fig. 6–III), which aims at capturing the obvious bi-layered structure of many mountain grasslands (e.g. Tappeiner and Cernusca, 1994), we further divided this single vegetation layer into two separate ones, within which phytoelements were again assumed to be distributed in a homogeneous manner. For this purpose the same heights as used for the model of wind speed (Table 1; Wohlfahrt et al., 2000) were adopted to separate the upper from the lower canopy layer. As can be seen from Fig. 6–III and IV, both simplifications produce considerable deviations in the resulting predictions, in particular for LE, H and A_C which are altered by up to 35%, indicating the importance of accounting for the vertical phytoelement distribution in heterogeneous (mountain grassland) canopies (Raupach and Finnigan, 1988; Tappeiner and Cernusca, 1998).

4. Conclusion

A model is presented which allows for simulating vegetation–atmosphere CO_2 and energy exchange of multi-component, multi-species grassland canopies, explicitly taking into account the structural and functional properties of the various components and species. For parameterisation a mixed approach is followed, using species-specific parameters for the components with the largest fractional contribution to the total biomass, and generic, average values for the remainder. The performance of the model in comparison with field measurements is broadly satisfactory, although validation of sensible and latent heat fluxes suffers from the difficulty to discern between the contributions from the soil and the vegetation. A sensitivity analysis reveals that the model is fairly sensitive to vegetation optical properties, indicating the need for own measurements, which were not available in the present study. The model was found to be less sensitive to soil optical properties, phytoelement inclination distributions and widths of the generic components, as well as bole respiration parameters. The latter finding though probably needs to be reconciled, if dwarf shrub dominated canopies are to be investigated. Using generic physiological parameters for the three main functional groups (forbs, graminoids and

dwarf shrubs), proved to produce acceptable results, despite a high sensitivity of the model to these parameters. This shows the potential of using the concept of functional groups for aggregating leaf physiological parameters, given a representative data basis exists. If predictions of bulk canopy exchange rates are of sole interest, assumption of a uniform spherical phytoelement angle distribution appears sufficient. Though, due to the distinct vertical heterogeneity of the investigated canopies considerable deviations in predicted bulk exchange rates are observed, if a vertical homogeneous distribution of phytoelements is assumed. Future model developments should aim at including the soil compartment (soil surface energy balance, soil water and heat transport, soil respiration), which would also ease model validation. Furthermore, it seems desirable to include turbulent transport of momentum, air temperature, water vapour and CO_2 concentration within and above the canopy.

Acknowledgements

Appendix A. Model of radiative transfer

Assuming that phytoelements are distributed at random, the probability that a ray of light incident at an angle (from the horizontal) β is intercepted in a layer j (counted from bottom upwards) by the phytoelements of a component p with a silhouette area of ΔL and inclined as described by an inclination distribution F, is given by (Goudriaan, 1977; Ross, 1981; Baldocchi

and Collineau, 1994)

$$P_i(p, j, \beta) = \frac{\Delta L(p, j)}{\sin \beta} \sum_{\lambda=1}^{9} F(p, j, \lambda) G(p, j, \beta, \lambda),$$

(A.1)

where G is the projection of the phytoelements inclined at an angle λ into the direction β (De Wit, 1965; Ross, 1981; Goudriaan, 1977), and may be calculated as

$$G(\beta, \lambda) = \sin \beta \cos \lambda \quad \text{if } \beta \geq \lambda,$$

(A.2)

$$G(\beta, \lambda) = \frac{2}{\pi} \left[\sin \beta \cos \lambda \arcsin \left(\frac{\tan \beta}{\tan \lambda} \right) + \sqrt{\sin^2 \lambda - \sin^2 \beta} \right] \quad \text{if } \beta < \lambda.$$

(A.3)

Because of the non-linear response of photosynthesis to PPFD the radiation incident on shaded and sunlit canopy areas must be considered separately. Shaded phytoelements receive diffuse light only, while sunlit ones receive both diffuse and direct radiation, the latter incident at an angle β^*, the elevation of the sun. The attenuation of beam radiation (Q_{dir}) is calculated as

$$Q_{dir}(j) = Q_{dir}(j + 1) - \sum_{p=1}^{np} Q_{dir}(j + 1) P_i(p, j, \beta^*),$$

(A.4)

where np stands for the number of phytoelements. The fraction of sunlit phytoelement area, f_{sl}, is proportional to the attenuation of direct radiation and hence given by

$$f_{sl}(j) = \frac{Q_{dir}(j + 1)}{Q_{dir}(n + 1)}$$

(A.5)

for $Q_{dir}(n + 1) > 0$, otherwise $f_{sl}(j) = 0$. The flux of diffuse radiation in the canopy consists of diffuse radiation from the atmosphere and of diffused, scattered beam radiation. For the treatment of diffuse radiation, the upper and lower hemispheres viewed by the phytoelements are divided into nine sectors of $10°$ each (due to this discretisation $\sin \beta$ in Eq. (A.1) needs to be replaced by $\frac{1}{2}[\sin(10\beta) + \sin(10(\beta - 1))]$ if nine sectors are distinguished; Jan Goudriaan, personal

communication). The downward short-wave fluxes (Q_d) within the canopy consist of the non-intercepted radiation from above (first part on the right-hand side of Eq. (A.6)), the diffuse radiation transmitted from above and reflected from below downwards (second part on the right-hand side of Eq. (A.6)), and the direct radiation transmitted in the downward direction (third part on the right-hand side of Eq. (A.6)) as

$$\begin{aligned} Q_d(j, \beta) &= Q_d(j + 1, \beta) - \sum_{p=1}^{np} P_i(p, j, \beta) Q_d(j + 1, \beta) \\ &+ \sum_{p=1}^{np} B_l(p, j, \beta') \sum_{\beta=1}^{9} P_i(p, j, \beta) \{Q_d(j + 1, \beta) \\ &\times [\xi(p, j, \beta, \beta')(\tau_c(p) - \rho_c(p)) + \rho_c(p)] \\ &+ Q_u(j - 1, \beta)[\xi(p, j, \beta, \beta') \\ &\times (\rho_c(p) - \tau_c(p)) + \tau_c(p)]\} \\ &+ \sum_{p=1}^{np} B_l(p, j, \beta') Q_{dir}(j + 1) P_i(p, j, \beta) \\ &\times [\xi(p, j, \beta, \beta')(\tau_c(p) - \rho_c(p)) + \rho_c(p)]. \end{aligned}$$

(A.6)

The prime (β') denotes that the angle refers to scattered radiation, ρ_c and τ_c are phytoelement reflection and transmission coefficients, respectively, and ξ is a reflection–transmission distribution function as defined by Goudriaan (1977). The scattered, i.e. reflected and transmitted, radiation, as well as emitted radiation, is distributed as

$$B_l(p, j, \beta') = \frac{B_u(\beta') P_i(p, j, \beta')}{\sum_{\beta=1}^{9} B_u(\beta) P_i(p, j, \beta)},$$

(A.7)

where B_u is the zonal distribution of radiation scattered by a lambertian reflector (Goudriaan, 1977), calculated for nine sky sectors as (Jan Goudriaan, personal communication)

$$B_u(\beta) = \sin(10\beta)^2 - \sin(10(\beta - 1))^2.$$

(A.8)

Similarly, the upward short-wave fluxes (Q_u) within the canopy consist of the non-intercepted radiation from below, the diffuse radiation transmitted from be-

low and reflected from above upwards, and the direct radiation reflected in the upward direction as

$$
\begin{aligned}
Q_u(j, \beta) &= Q_u(j-1, \beta) - \sum_{p=1}^{np} P_i(p, j, \beta) Q_u(j-1, \beta) \\
&+ \sum_{p=1}^{np} B_l(p, j, \beta') \sum_{\beta'=1}^{9} P_i(p, j, \beta)\{Q_d(j+1, \beta) \\
&\times [\xi(p, j, \beta, \beta')(\rho_c(p) - \tau_c(p)) + \tau_c(p)] \\
&+ Q_u(j-1, \beta)[\xi(p, j, \beta, \beta') \\
&\times (\tau_c(p) - \rho_c(p)) + \rho_c(p)]\} \\
&+ \sum_{p=1}^{np} B_l(p, j, \beta') Q_{dir}(j+1) P_i(p, j, \beta) \\
&\times [\xi(p, j, \beta, \beta')(\rho_c(p) - \tau_c(p)) + \tau_c(p)]. \quad (A.9)
\end{aligned}
$$

When calculating the within-canopy profile of long-wave radiation it has to be accounted for that the phytoelements themselves emit long-wave radiation. Since leaves do not transmit long-wave radiation ($\tau_c = 0$), the calculation of the downward and upward fluxes is considerably simpler as compared to Eqs. (A.6) and (A.9), i.e.

$$
\begin{aligned}
L_d(j, \beta) &= L_d(j+1, \beta) - \sum_{p=1}^{np} P_i(p, j, \beta) L_d(j+1, \beta) \\
&+ \rho_c(p) B_l(p, j, \beta') \sum_{p=1}^{np} P_i(p, j, \beta) L_u \\
&\times (j-1, \beta) + \varepsilon_c(p)\beta_l(p, j, \beta')\Delta L \\
&\times (p, j)\sigma[T_{pKsl}(p, j)^4 f_{sl}(j) \\
&+ T_{pKsh}(p, j)^4 (1 - f_{sl}(j))], \quad (A.10)
\end{aligned}
$$

$$
\begin{aligned}
L_u(j, \beta) &= L_u(j-1, \beta) - \sum_{p=1}^{np} P_i(p, j, \beta) L_u(j-1, \beta) \\
&+ \rho_c(p) B_l(p, j, \beta') \sum_{p=1}^{np} P_i(p, j, \beta) L_d \\
&\times (j+1, \beta) + \varepsilon_c(p)\beta_l(p, j, \beta')\Delta L \\
&\times (p, j)\sigma[T_{pKsl}(p, j)^4 f_{sl}(j) \\
&+ T_{pKsh}(p, j)^4 (1 - f_{sl}(j))]. \quad (A.11)
\end{aligned}
$$

The downward (Eq. (A.10)) and upward (Eq. (A.11)) fluxes of long-wave radiation thus consist of the non-intercepted flux from above and below, respectively, the upward radiation reflected downwards and the downward radiation reflected upwards, respectively, and the emitted radiation. The latter is calculated as the weighted mean flux from sunlit and shaded phytoelements, which radiate at absolute temperatures T_{pKsl} and T_{pKsh}, respectively, using the Stefan–Boltzman law. Emissivity ε_c is assumed to be equal to $(1 - \rho_c)$ (Kirchhoff's law).

At the soil surface, the lower boundary condition of the model, light is reflected/emitted lambertian as

$$
Q_u(0, \beta) = \rho_s B_u(\beta') \sum_{\beta=1}^{9} Q_d(1, \beta)
$$
for short-wave radiation, (A.12)

$$
L_u(0, \beta) = B_u(\beta) \left[(1 - \rho_s)\sigma T_{sK}^4 + \rho_s \sum_{\beta=1}^{9} L_d(1, \beta) \right]
$$
for long-wave radiation, (A.13)

where ρ_s is the wavelength-dependent soil reflection coefficient and T_{sK} the absolute soil surface temperature.

The soil and the sky emitted long-wave radiation, as well as the short-wave radiation, represent state variables, the corresponding radiation fields are hence calculated only once per time step. Whereas the long-wave radiation emitted by the phytoelements depends upon their temperatures and in turn influences their temperatures via the energy balance (Eq. (5)), making it necessary to solve in an iterative fashion for their equilibrium temperatures.

Now that the within-canopy radiation field has been specified, it is possible to calculate the amount of radiation intercepted and/or absorbed by the various canopy components. Short-wave radiation incident on shaded phytoelements is calculated as

$$
\begin{aligned}
Q_{shade}(p, j) = \sum_{\beta=1}^{9} \left[\frac{G(p, j, \beta, \lambda)}{\sin \beta} (Q_d(j+1, \beta) \right. \\
\left. + Q_u(j-1, \beta)) \right], \quad (A.14)
\end{aligned}
$$

and the radiation incident on sunlit phytoelements is given by

$$Q_{\text{sun}}(p, j) = Q_{\text{shade}}(p, j) + Q_{\text{dir}}(n + 1) \frac{G(p, j, \beta, \lambda)}{\sin \beta^*}, \qquad (A.15)$$

where $Q_{\text{dir}}(n + 1)$ stands for the direct radiation measured on a horizontal plane above the canopy. Long-wave radiation is distributed equally among sunlit and shaded canopy components as

$$L(p, j) = \sum_{\beta=1}^{9} \left[\frac{G(p, j, \beta^*, \lambda)}{\sin \beta} (L_d(j + 1, \beta) + L_u(j - 1, \beta)) \right]. \qquad (A.16)$$

The results of Eqs. (A.14) and (A.15) may be used directly to calculate assimilation, since PPFD in the leaf gas exchange model (Eq. (6) in Wohlfahrt et al., 1998) refers to an incident light basis. In order to calculate absorbed short-wave and long-wave radiation, as it is required for the leaf energy balance (Eq. (5)), Q_{shade}, Q_{sun} and L need to be multiplied by an absorption coefficient, which is calculated as $(1 - (\rho_c + \tau_c))$.

Solar geometry, determining the position of the sun in the sky, is calculated using the equations given in Campbell and Norman (1998). Total solar radiation, as well as the partitioning of solar radiation into direct and diffuse, PPFD and NIR components, is either modelled using the approach described in Goudriaan (1977) and Goudriaan and Van Laar (1994), or measured values (as described in the previous section) are used instead. Similarly, sky long-wave radiation may be either estimated using the equations by Brutsaert (1984) and Monteith and Unsworth (1990), or measured values be used. The corresponding algorithms have been presented in Wohlfahrt et al. (2000).

References

Anderson, M.C., Norman, J.M., Meyers, T.P., Diak, G.R., 2000. An analytical model for estimating canopy transpiration and carbon assimilation fluxes based on canopy light-use efficiency. Agric. For. Meteorol. 101, 265–289.

Anthoni, P.M., Law, B.E., Unsworth, M.H., 1999. Carbon and water vapor exchange of an open-canopied ponderosa pine ecosystem. Agric. For. Meteorol. 95, 151–168.

Asner, G.P., Wessman, C.A., 1997. Scaling PAR absorption from the leaf to landscape level in spatially heterogeneous ecosystems. Ecol. Model. 103, 81–97.

Asner, G.P., Wessman, C.A., Schimel, D.S., Archer, S., 1998a. Variability in leaf and litter optical properties: implications for BRDF model inversions using AVHRR, MODIS, and MISR. Remote Sens. Environ. 63, 243–257.

Asner, G.P., Wessman, C.A., Archer, S., 1998b. Scale dependence of absorption of photosynthetically active radiation in terrestrial ecosystems. Ecol. Appl. 8, 1003–1021.

Bahn, M., Cernusca, A., Tappeiner, U., Tasser, E., 1994. Wachstum krautiger Arten auf einer Mähwiese und einer Almbrache. Ver. Ges. Ökol. 23, 23–30.

Bahn, M., Wohlfahrt, G., Haubner, E., Horak, I., Michaeler, W., Rottmar, K., Tappeiner, U., Cernusca, A., 1999. Leaf photosynthesis, nitrogen contents and specific leaf area of grassland species in mountain ecosystems under different land use. In: Cernusca, A., Tappeiner, U., Bayfield, N. (Eds.), Land-use Changes in European Mountain Ecosystems. ECOMONT — Concepts and Results. Blackwell Wissenschafts-Verlag, Berlin, pp. 247–255.

Baldocchi, D.D., 1992. A Lagrangian random walk model for simulating water vapor, CO_2 and sensible heat flux densities and scalar profiles over and within a soybean canopy. Boundary Layer Meteorol. 61, 113–144.

Baldocchi, D.D., 1993. Scaling water vapor and carbon dioxide exchange from leaves to canopy: rules and tools. In: Ehleringer, J.R., Field, C.B. (Eds.), Scaling Physiological Processes: Leaf to Globe. Academic Press, San Diego, CA, pp. 77–116.

Baldocchi, D.D., Collineau, S., 1994. The physical nature of solar radiation in heterogeneous canopies: spatial and temporal attributes. In: Caldwell, M.M., Pearcy, R.W. (Eds.), Exploitation of Environmental Heterogeneity by Plants. Academic Press, San Diego, CA, pp. 21–71.

Baldocchi, D.D., Harley, P.C., 1995. Scaling carbon dioxide and water vapor exchange from leaf to canopy in a deciduous forest. II. Model testing and application. Plant Cell Environ. 18, 1157–1173.

Baldocchi, D.D., Meyers, T., 1998. On using eco-physiological, micrometeorological and biogeochemical theory to evaluate carbon dioxide, water vapor and trace gas fluxes over vegetation: a perspective. Agric. For. Meteorol. 90, 1–25.

Ball, J.T., Woodrow, I.E., Berry, J.A., 1987. A model predicting stomatal conductance and its contribution to the control of photosynthesis under different environmental conditions. In: Biggens, J. (Ed.), Progress in Photosynthesis Research, Vol. IV. Proceedings of the VII International Congress on Photosynthesis. Martinus Nijhoff, Dordrecht, pp. 221–224.

Baumgardner, M.F., Silva, L.F., Biehl, L.L., Stoner, E.R., 1985. Reflectance properties of soils. Adv. Agron. 38, 1–44.

Berry, J.A., Collatz, G.J., Denning, A.S., Colello, G.D., Fu, W., Grivet, C., Randall, D.A., Sellers, P.J., 1998. SiB2, a model for simulation of biological processes within a climate model. In: Van Gardingen, P.R., Foody, G.M., Curran, P.J. (Eds.), Scaling-up: From Cell to Landscape. Society of Experimental Biology Seminar Series 63. Cambridge University Press, Cambridge, pp. 347–369.

Brutsaert, W., 1984. Evaporation into the Atmosphere: Theory, History, and Applications. Reidel, Boston, MA.

Campbell, G.S., 1985. Soil Physics with BASIC. Elsevier, Amsterdam.

Campbell, G.S., Norman, J.M., 1998. An Introduction to Environmental Biophysics, 2nd Edition. Springer, New York.

Cernusca, A., 1987. Application of computer methods in the field to assess ecosystem function and response to stress. In: Tenhunen, J.D., Catarino, F.M., Lange, O.L., Oechel, W.C. (Eds.), Plant Response to Stress. NATO ASI Series, Vol. G15. Springer, Berlin, pp. 157–164.

Cernusca, A., 1991. Batteriebetriebenes Thermoelemente-Aspirationspsychrometer für Mikroklima- und Energiehaushaltsuntersuchungen. In: Wieser, W., Cernusca, A. (Eds.), Entwicklung und Einsatz neuer wissenschaftlicher Geräte und Methoden. Veröffentlichungen der Universität Innsbruck 181, Innsbruck, pp. 14–18.

Cernusca, A., Decker, P., 1989. Vergleichende Atmungsmessungen an Graslandökosystemen. In: Cernusca, A. (Ed.), Struktur und Funktion von Graslandökosystemen in Nationalpark Hohe Tauern. Universitätsverlag Wagner, Innsbruck, pp. 405–417.

Cernusca, A., Seeber, M.C., 1981. Canopy structure, microclimate and the energy budget in different alpine plant communities. In: Grace, J., Ford, E.D., Jarvis, P.G. (Eds.), Plants and their Atmospheric Environment. 21st Symposium of the British Ecological Society. Blackwell, Oxford, pp. 75–81.

Cernusca, A., Tappeiner, U., Agostini, A., Bahn, M., Bezzi, A., Egger, R., Kofler, R., Newesely, C., Orlandi, D., Prock, S., Schatz, H., Schatz, I., 1992. Ecosystem research on mixed grassland/woodland ecosystems. First results of the EC-STEP-project INTEGRALP on Mt. Bondone. Studi Trentini Di Science Naturali. Acta Biol. 67, 99–133.

Cernusca, A., Bahn, M., Chemini, C., Graber, W., Siegwolf, R., Tappeiner, U., Tenhunen, J., 1998. ECOMONT: a combined approach of field measurements and process-based modelling for assessing effects of land-use changes in mountain landscapes. Ecol. Model. 113, 167–178.

Cescatti, A., Chemini, C., De Siena, C., Gianelle, D., Nicolini, G., Wohlfahrt, G., 1999. Monte Bondone composite landscape, Italy. In: Cernusca, A., Tappeiner, U., Bayfield, N. (Eds.), Land-use Changes in European Mountain Ecosystems. ECOMONT — Concepts and Results. Blackwell Wissenschafts-Verlag, Berlin, pp. 60–73.

Chapin III, F.S., 1993. Functional role of growth forms in ecosystem and global processes. In: Ehleringer, J.R., Field, C.B. (Eds.), Scaling Physiological Processes: Leaf to Globe. Academic Press, San Diego, CA, pp. 287–312.

Chen, J.M., Liu, J., Cihlar, J., Goulden, M.L., 1999. Daily canopy photosynthesis model through temporal and spatial scaling for remote sensing applications. Ecol. Model. 124, 99–119.

Cox, P.M., Huntingford, C., Harding, R.J., 1998. A canopy conductance and photosynthesis model for use in a GCM land surface scheme. J. Hydrol. 212–213, 79–94.

Dawson, T.E., Chapin III, F.S., 1993. Grouping plants by their form-function characteristics as an avenue for simplification in scaling between leaves and landscapes. In: Ehleringer, J.R., Field, C.B. (Eds.), Scaling Physiological Processes: Leaf to Globe. Academic Press, San Diego, CA, pp. 313–322.

De Pury, D.G.G., Farquhar, G.D., 1997. Simple scaling of photosynthesis from leaves to canopies without the errors of big-leaf models. Plant Cell Environ. 20, 537–557.

De Wit, C.T., 1965. Photosynthesis of leaf canopies. Agricultural Research Report No. 663. Pudoc, Wageningen.

Droppo, J.G., Hamilton, H.L., 1973. Experimental variability in the determination of the energy balance in a deciduous forest. J. Appl. Meteorol. 12, 781–791.

Ehleringer, J.R., Field, C.B. (Eds.), 1993. Scaling Physiological Processes: Leaf to Globe. Academic Press, San Diego, CA.

Falge, E., Graber, W., Siegwolf, R., Tenhunen, J.D., 1996. A model of the gas exchange of *Picea abies* to habitat conditions. Trees 10, 277–287.

Farquhar, G.D., 1979. Models describing the kinetics of ribulose bisphosphate carboxylase–oxygenase. Arch. Biochem. Biophys. 193, 456–468.

Farquhar, G.D., Sharkey, T.D., 1982. Stomatal conductance and photosynthesis. Ann. Rev. Plant Physiol. 33, 317–342.

Farquhar, G.D., Von Caemmerer, S., 1982. Modelling of photosynthetic response to environmental conditions. In: Lange, O.L., Nobel, P.S., Osmond, C.B., Ziegler, H. (Eds.), Physiological Plant Ecology, Vol. II. Encyclopedia of Plant Physiology, Vol. 12B. Springer, Berlin, pp. 549–588.

Farquhar, G.D., Von Caemmerer, S., Berry, J.A., 1980. A biochemical model of photosynthetic CO_2 assimilation in leaves of C_3 species. Planta 149, 78–90.

Finnigan, J.J., Raupach, M.R., 1987. Transfer processes in plant canopies in relation to stomatal characteristics. In: Zeiger, E., Farquhar, G.D., Cowan, I.R. (Eds.), Stomatal Function. Stanford University Press, Stanford, CA, pp. 385–429.

Gandolfo, C., Sulli, M., 1993. Studi sul clima del Trentino per ricerche dendroclimatologiche e di ecologia forestale. Provincia Autonoma di Trento-Servizio Foreste, Caccia e Pesca.

Gazarini, L.C., 1988. Bestandesstruktur und Strahlungsextinktion von Zwergstrauch-beständen (*Vaccinium myrtillus* L. und *Rhododendron ferrugineum* L.) an der alpinen Waldgrenze. Ph.D. Thesis. University of Innsbruck, Innsbruck.

Goudriaan, J., 1977. Crop micrometeorology: a simulation study. Simulation Monographs. Centre for Agricultural Publishing and Documentation, Pudoc, Wageningen.

Goudriaan, J., Van Laar, H.H., 1994. Modelling Crop Growth Processes. Kluwer Academic Publishers, Amsterdam.

Halldin, S., Lindroth, A., 1992. Errors in net radiometry: comparison and evaluation of six radiometer designs. J. Atmos. Ocean. Technol. 9, 762–783.

Harley, P.C., Tenhunen, J.D., 1991. Modeling the photosynthetic response of C_3 leaves to environmental factors. In: Boote, K.J., Loomis, R.S. (Eds.), Modeling Crop Photosynthesis — From Biochemistry to Canopy. CSSA Special Publication No. 19. American Society of Agronomy and Crop Science Society of America, Madison, WI, pp. 17–39.

Jacquemoud, S., Baret, F., Hanocq, J.F., 1992. Modeling spectral and bidirectional soil reflectance. Remote Sens. Environ. 41, 123–132.

Jordan, D.B., Ogren, W.L., 1984. The CO_2/O_2 specificity of ribulose-1,5-bisphosphate carboxylase/oxygenase. Dependence on ribulose-bisphosphate concentration, pH and temperature. Planta 161, 308–313.

Kellomäki, S., Wang, K.-Y., 1999. Short-term environmental controls of heat and water vapour fluxes above a boreal coniferous forest: model computations compared with measurements by eddy correlation. Ecol. Model. 124, 145–173.

Leuning, R., Kelliher, F.M., De Pury, D.G.G., Schulze, E.D., 1995. Leaf nitrogen, photosynthesis, conductance and transpiration: scaling from leaves to canopies. Plant Cell Environ. 18, 1183–1200.

Lloyd, J., 1999. Current perspectives on the terrestrial carbon cycle. Tellus Ser. B 51, 336–342.

Medlyn, B.E., Badeck, F.-W., De Pury, D.G.G., Barton, C.V.M., Broadmeadow, M., Ceulemans, R., De Angelis, P., Forstreuter, M., Jach, M.E., Kellömaki, S., Laitat, E., Marek, M., Philipott, S., Rey, A., Strassemeyer, J., Laitinen, K., Liozon, R., Portier, B., Roberntz, P., Wang, K., Jarvis, P.G., 1999. Effects of elevated [CO_2] on photosynthesis in European forest species: a meta-analysis of model parameters. Plant Cell Environ. 22, 1475–1495.

Monsi, M., Saeki, T., 1953. Über den Lichtfaktor in den Pflanzengesellschaften und seine Bedeutung für die Stoffproduktion. Jpn. J. Bot. 14, 22–52.

Monteith, J.L., 1957. Dew. Quart. J. R. Met. Soc. 83, 161–168.

Monteith, J.L., 1977. Principles of Environmental Physics, 1st Edition. Edward Arnold, London.

Monteith, J.L., Unsworth, M.H., 1990. Principles of Environmental Physics, 2nd Edition. Edward Arnold, London.

Niinemets, Ü., 1999. Components of leaf dry mass per area — thickness and density — alter leaf photosynthetic capacity in reverse directions in woody plants. New Phytol. 144, 35–47.

Nikolov, N.T., Massman, W.J., Schoettle, A.W., 1995. Coupling biochemical and biophysical processes at the leaf level: an equilibrium photosynthesis model for leaves of C_3 plants. Ecol. Model. 80, 205–235.

Nobel, P.S., 1991. Physicochemical and Environmental Plant Physiology. Academic Press, San Diego, CA.

Pachepsky, L.B., Haskett, J.D., Acock, B., 1996. An adequate model of photosynthesis. I. Parameterization, validation and comparison of models. Agric. Syst. 50, 209–225.

Paw U, K.T., 1987. Mathematical analysis of the operative temperature and energy budget. J. Therm. Biol. 12, 227–233.

Raupach, M.R., Finnigan, J.J., 1988. Single-layer models of evaporation from plant canopies are incorrect but useful, whereas multilayer models are correct but useless: discuss. Aust. J. Plant Physiol. 15, 705–716.

Raupach, M.R., Finkele, K., Zhang, L., 1997. SCAM (soil-canopy–atmosphere model): description and comparison with field data. Technical Report No. 132. Centre for Environmental Mechanics, CSIRO.

Reich, P.B., Ellsworth, D.S., Walters, M.B., 1998a. Leaf structure (SLA) modulates photosynthesis relations: evidence from within and across species, functional groups, and biomes. Funct. Ecol. 12, 948–958.

Reich, P.B., Walters, M.B., Ellsworth, D.S., Vose, J.M., Volin, J.C., Gresham, C., Bowman, W.D., 1998b. Relationship of leaf dark respiration to leaf nitrogen, specific leaf area and leaf life span: a test across biomes and functional groups. Oecologia 114, 471–482.

Ross, J., 1981. The Radiation Regime and Architecture of Plant Stands. Junk Publisher, The Hague.

Running, S.W., Baldocchi, D.D., Turner, D.P., Gower, S.T., Bakwin, P.S., Hibbard, K.A., 1999. A global terrestrial monitoring network integrating tower fluxes, flask sampling, ecosystem modelling and EOS satellite data. Remote Sens. Environ. 70, 108–127.

Rutter, A.J., 1979. The hydrological cycle in vegetation. In: Monteith, J.L. (Ed.), Vegetation and Atmosphere, Vol. 1. Academic Press, London, pp. 111–154.

Sage, R.F., 1994. Acclimation of photosynthesis to increasing atmospheric CO_2: the gas exchange perspective. Photosynth. Res. 39, 351–368.

Siegwolf, R., 1987. CO_2-Gaswechsel von *Rhododendron ferrugineum* L. im Jahresgang an der Alpinen Waldgrenze. Ph.D. Thesis. University of Innsbruck, Innsbruck.

Sinoquet, H., Rakocevic, M., Varlet-Grancher, C., 2000. Comparison of models for day light partitioning in multispecies canopies. Agric. For. Meteorol. 101, 251–263.

Smith, E.A., Hodges, G.B., Bacrania, M., Cooper, H.J., Owens, M.A., Chappel, R., Kincannon, W., 1997. BOREAS net radiometer engineering study. NASA-Goddard Space Flight Center, Greenbelt, USA.

Spatz, G., Weiss, G.B., Dolar, D.M., 1978. Der Einfluß der Bewirtschaftungsänderungen auf die Vegetation von Almen im Gasteiner Tal. In: Cernusca, A. (Ed.), Ökologische Analysen von Almflächen im Gasteinertal. Veröffentlichungen des Österreichischen MaB-Hochgebirgsprogramms in den Hohen Tauern, Bd. 2, Wagner, Innsbruck, pp. 163–180.

Steffen, W., Noble, I., Canadell, J., Apps, M., Schulze, E.-D., Jarvis, P.G., Baldocchi, D., Ciais, P., Cramer, W., Ehleringer, J., Farquhar, G., Field, C.B., Ghazi, A., Gifford, R., Heimann, M., Houghton, R., Kabat, P., Körner, Ch., Lambin, E., Linder, S., Mooney, H.A., Murdiyarso, D., Post, W.M., Prentice, C., Raupach, M.R., Schimel, D.S., Shvidenko, A., Valentini, R., 1998. The terrestrial carbon cycle: implications for the Kyoto protocol. Science 280, 1393–1394.

Tappeiner, U., Cernusca, A., 1994. Bestandesstruktur, Energie-haushalt und Bodenatmung einer Mähwiese, einer Almweide und einer Almbrache. Ver. Ges. Ökol. 23, 49–56.

Tappeiner, U., Cernusca, A., 1995. Analysis of changes in canopy structure and microclimate in abandoned alpine grassland ecosystems. In: Bellan, D., Bonin, G., Emig, C. (Eds.), Functioning and Dynamics of Natural and Perturbed Ecosystems. Lavoisier Publishing, Paris, pp. 49–62.

Tappeiner, U., Cernusca, A., 1996. Microclimate and fluxes of water vapour, sensible heat and carbon dioxide in structurally differing subalpine plant communities in the Central Caucasus. Plant Cell Environ. 19, 403–417.

Tappeiner, U., Cernusca, A., 1998. Model simulation of spatial distribution of photosynthesis in structurally differing plant communities in the Central Caucasus. Ecol. Model. 113, 201–223.

Tappeiner, U., Sapinsky, S., 1999. Canopy structure, primary production and litter decomposition. In: Cernusca, A., Tappeiner, U., Bayfield, N. (Eds.), Land-use Changes in European Mountain Ecosystems. ECOMONT — Concepts and Results. Blackwell Wissenschafts-Verlag, Berlin, pp. 127–129.

Tappeiner, U., Cernusca, A., Siegwolf, R.T.W., Sapinsky, S., Newesely, Ch., Geissbühler, P., Stefanicki, G., 1999. Microclimate, energy budget and CO_2 gas exchange of ecosystems. In: Cernusca, A., Tappeiner, U., Bayfield, N. (Eds.), Land-use Changes in European Mountain Ecosystems. ECOMONT — Concepts and Results. Blackwell Wissenschafts-Verlag, Berlin, pp. 135–145.

Tasser, E., Prock, S., Mulser, J., 1999. Impact of land use on vegetation along the Eastern Alpine transect. In: Cernusca, A., Tappeiner, U., Bayfield, N. (Eds.), Land-use Changes in European Mountain Ecosystems. ECOMONT — Concepts and Results. Blackwell Wissenschafts-Verlag, Berlin, pp. 235–246.

Tenhunen, J.D., Siegwolf, R.T.W., Oberbauer, S.F., 1994. Effects of phenology, physiology, and gradients in community composition, structure, and microclimate on tundra ecosystem CO_2 exchange. In: Schulze, E.-D., Caldwell, M.M. (Eds.), Ecophysiology of Photosynthesis. Ecol. Studies, Vol. 100. Springer, Heidelberg, pp. 431–460.

Van Gardingen, P.R., Foody, G.M., Curran, P.J. (Eds.), 1997. Scaling-up: From Cell to Landscape. Society of Experimental Biology Seminar Series 63. Cambridge University Press, Cambridge.

Wang, Y.-P., Leuning, R., 1998. A two-leaf model for canopy conductance, photosynthesis and partitioning of available energy. I. Model description and comparison with a multi-layered model. Agric. For. Meteorol. 91, 89–111.

Wenhan, Q., 1993. Modelling bidirectional reflectance of multicomponent vegetation canopies. Remote Sens. Environ. 46, 235–245.

Williams, M., Rastetter, E.B., Fernandes, D.N., Goulden, M.L., Wofsy, S.C., Shaver, G.R., Melillo, J.M., Munger, J.W., Fan, S.-M., Nadelhoffer, K.J., 1996. Modelling the soil–plant–atmosphere continuum in a *Quercus-Acer* stand at Harvard forest: the regulation of stomatal conductance by light, nitrogen and soil/plant hydraulic properties. Plant Cell Environ. 19, 911–927.

Wilson, T.B., Bland, W.L., Norman, J.M., 1999. Measurement and simulation of dew accumulation and drying in a potato canopy. Agric. For. Meteorol. 93, 111–119.

Wohlfahrt, G., Bahn, M., Horak, I., Tappeiner, U., Cernusca, A., 1998. A nitrogen sensitive model of leaf carbon dioxide and water vapour gas exchange: application to 13 key species from differently managed mountain grassland ecosystems. Ecol. Model. 113, 179–199.

Wohlfahrt, G., Bahn, M., Haubner, E., Horak, I., Michaeler, W., Rottmar, K., Tappeiner, U., Cernusca, A., 1999. Inter-specific variation of the biochemical limitation to photosynthesis and related leaf traits of 30 species from mountain grassland differing in land use. Plant Cell Environ. 22, 1281–1296.

Wohlfahrt, G., Bahn, M., Tappeiner, U., Cernusca, A., 2000. A model of whole plant gas exchange for herbaceous species from mountain grassland sites differing in land use. Ecol. Model. 125, 173–201.

Wullschleger, S.D., 1993. Biochemical limitations to carbon assimilation in C_3 plants — a retrospective analysis of the A/C_i curves from 109 species. J. Exp. Bot. 44, 907–920.